

Bridge River Archaeological Project Geophysical Investigations

Phase II – Final Report



Prepared for:
**Department of Anthropology
University of Montana
Missoula, MT 59812-1001**

**Project: 05 -13
28 July, 2005**

Terrascan Geophysics
4506 West 4th Avenue
Vancouver, British Columbia, Canada V6R 1R3
Tel/Fax: (604) 221-2400
www.terrascan.ca



Terrascan Geophysics
4506 West 4th Avenue
Vancouver, British Columbia, Canada V6R 1R3
Tel/Fax: (604) 221-2400
www.terrascan.ca



Bridge River Archaeological Project Geophysical Investigations

Phase II – Final Report

Prepared for:

Department of Anthropology
University of Montana
Missoula, MT 59812-1001

Attention:

Dr. William Prentiss

Distribution:

28 July, 2005

1 copy – University of Montana
1 copy – Bridge River Band
1 copy – Terrascan Geophysics

TABLE OF CONTENTS

<u>SECTION</u>	<u>PAGE</u>
1.0 BACKGROUND - SCOPE OF WORK.....	1
2.0 METHODS	2
2.1 Electromagnetic Terrain Conductivity.....	2
2.2 Magnetic Gradient	2
2.4 Ground Penetrating Radar	4
3.0 RESULTS.....	5
3.1 HP24/HP36.....	5
3.2 HP20.....	6
3.3 HP10/11.....	7
3.4 HP54.....	9
4.0 CONCLUDING REMARKS	10
5.0 REFERENCE	12

LIST OF FIGURES

Figure 1	Location Plan – Aerial Site Photo
Figure 2	Phase I – Apparent Conductivity
Figure 3	Phase I – Magnetic Gradient
Figure 4	Geonics EM-31/EM-38 Characteristics
Figure 5	Vertical Electrical Soundings
Figure 6	EPF Magnetic Signatures – Plan
Figure 7	EPF Magnetic Signatures – Profile
Figure 8	GPR 3-D Resampling Process
Figure 9	HP24/HP36 Magnetic – Conductivity
Figure 10	HP24/HP36 Magnetic – GPR Raw 0.0-1.0 m
Figure 11	HP24/HP36 Magnetic – GPR Absolute 0.0-1.0 m
Figure 12	HP24/HP36 Magnetic – GPR Raw 1.0-2.0 m
Figure 13	HP24/HP36 Magnetic – GPR Absolute 1.0-2.0 m
Figure 14	HP20 Magnetic – Conductivity
Figure 15	HP20 Magnetic – GPR Raw 0.0-1.0 m
Figure 16	HP20 Magnetic – GPR Absolute 0.0-1.0 m
Figure 17	HP20 Magnetic – GPR Raw 1.0-2.0 m
Figure 18	HP20 Magnetic – GPR Absolute 1.0-2.0 m
Figure 19	HP10/11 Magnetic – Conductivity
Figure 20	HP10/11 Magnetic – GPR Raw 0.0-1.0 m
Figure 21	HP10/11 Magnetic – GPR Absolute 0.0-1.0 m
Figure 22	HP10/11 Magnetic – GPR Raw 1.0-2.0 m
Figure 23	HP10/11 Magnetic – GPR Absolute 1.0-2.0 m
Figure 24	HP54 GPR Scan – 2004 Excavation Trench
Figure 25	HP54 GPR Scans

1.0 BACKGROUND - SCOPE OF WORK

A multiphase geophysical investigation of the Bridge River site (EeRI 4 – Figure 1) was initiated in June 2003 in coordination with preliminary archaeological excavations and related dating of recovered materials. As previously reported (Cross, 2004), an initial phase of geophysical investigations entailed site-wide surveys to map known and previously unidentified features and to guide subsequent archaeological sampling and interpretation. Phase I results are summarized in Figures 2 and 3, depicting the spatial variability of electrical conductivity and vertical magnetic gradient, respectively.

In addition to establishing a generally consistent geophysical signature in connection with pit house features, preliminary investigations also revealed potentially significant and meaningful variability from house to house. To further resolve and define the patterned distribution and variability of detected and more subtle features, Phase II geophysical investigations, involved the acquisition of higher-density measurements within and surrounding selected house floors. In particular, high-resolution surveys, utilizing electromagnetic (EM) conductivity, gradient magnetic and ground penetrating radar (GPR) methods were carried out within the three areas outlined in Figures 1 and 2. Compared with a 1.0 - 2.0 m sample interval employed for site-wide reconnaissance, the sample interval for Phase II focused investigations did not exceed 0.5 m.

Beyond direct archaeological interpretation of resulting data, it is anticipated that Phase II results will subsequently be calibrated via coincident large-area excavation to confirm and establish direct correspondence between patterned geophysical signatures and related archaeological deposits. In addition to verifying the archaeological significance of associated geophysical signatures, resulting calibration would provide a basis for subsequent interpretation of similar signatures with enhanced confidence and reliability.

As per Figures 2 and 3, Phase II investigations were undertaken with reference to the existing 20 m x 20 m reference grid, as established in 2003. Following clearance of surface vegetation within delineated survey areas, temporary reference marks were placed at 1.0 x 1.0 m intervals. Phase II fieldwork was conducted during the period September – December, 2004.

Finally, in addition to planned Phase II investigations, limited ground radar reconnaissance was conducted within HP54 to assist in the assessment of preliminary archaeological excavations and related dating.

For a brief discussion of geophysical methodologies see (Cross, 2004). Subsequent sections provide a factual description of specific procedures and findings for Phase II investigations.

2.0 METHODS / PROCEDURES

2.1 Electromagnetic Terrain Conductivity

To provide enhanced spatial resolution, EM conductivity measurements were acquired via a Geonics EM-38 terrain conductivity meter. In contrast with the Geonics EM-31, utilized for Phase I site-wide reconnaissance, the horizontal offset between transmitter (Tx) and receiver (Rx) coils (Figure 4) is substantially reduced, providing a more focused subsurface measurement. In particular, as tabulated in Figure 4 for vertical-dipole mode, a Tx-Rx offset of 1.0 m for the EM-38 reduces the effective measurement range to approximately 1.5 m, compared with roughly 5.5 m for the EM-31, with a Tx-Rx offset of 3.7 m.

In all cases, conductivity measurements were acquired at 0.5 m intervals, with the instrument at ground level and parallel to east-west transects separated by 0.5 m. Surveys were initiated from the southeast grid corner.

Measurements and associated grid coordinates were digitally recorded via an Omnidata DL-720 data logger and subsequently downloaded to a portable field computer for processing and analysis.

To constrain absolute electrical conductivity levels and related time-dependent variation, repeat vertical electrical soundings were acquired at HP57 in connection with Phase I and Phase II surveys. In each instance, two soundings were acquired on north-south transects; VES-1 on the west rim of HP57 (approximately along the 0E baseline) and VES-2 centered within the floor of HP57. As anticipated, results displayed in Figure 5 indicate that near-surface soil conditions were generally more conductive during Phase II investigations, carried out under relatively cool and moist autumn conditions. Relatively resistive conditions at depth for VES-2 presumably reflect the continued influence of unusually dry conditions during previous summer (2004) months.

2.2 Magnetic Gradient

To define optimum acquisition parameters for Phase II magnetic investigations, a series of experimental mappings were acquired over a well-defined external pit feature (EPF) centered at approximately 0E,106N on the northern rim of HP20. Figure 6 displays measured total field and vertical gradient distributions

for lower sensor heights of 0.3 m and 0.5 m (sensor midpoint) above local grade. Related anomaly profiles are presented in Figure 7. Total field is measured at the lower sensor and vertical sensor offset is 0.5 m. As anticipated, optimum definition of magnetic variability is provided by vertical gradient measurement with sensors positioned nearer local grade. Consequently, given no indication of excessive gradients or signal decay rates, subsequent Phase II magnetic surveys were conducted in vertical gradient mode with sensors located approximately 0.3 m and 0.8 m above grade.

In general, the characteristics of magnetic signatures presented in Figures 6 and 7 are contrary to expectation for induced magnetization associated with a concentrated source of magnetically susceptible material at mid-high magnetic latitude. It is possible that consistent apparent polarity reversal is attributable to remanent magnetization of EPF deposits or that the signature reflects the removal and redeposition of magnetically enhanced soils surrounding the pit feature. It is planned to further investigate the nature of related deposits and the precise attributes of associated geophysical signatures in connection with future excavations and model experiments. However, for present purposes, identification of anomalous signatures, their spatial distribution and patterning is the primary objective.

Phase II magnetic surveys focusing on HP24 were acquired via a Scintrex-EDA OMNI IV proton precession gradiometer as employed for the Phase I site-wide investigation. To facilitate more extensive coverage surrounding HP20 and to provide independent confirmation of previously recorded magnetic signatures, Phase II measurements in the vicinity of HP11 and HP20 were acquired utilizing a Geometrics G-858 caesium vapour gradiometer. Compared with a 3-5 s measurement cycle for the OMNI IV, the G-858 provides cycle rates to 10 /s with comparable sensitivity. A drawback of the G-858, however, is that the sensor staff configuration locates the detectors significantly forward of the operator, limiting precise control of sensor height and orientation in connection with local topographic relief. Although related localized error could be significant in the case of the HP11, these effects were minimized in connection with the HP20 survey via a non-magnetic reference height locator to maintain the lower sensor at 0.3 m above local grade.

Abnormal readings at several locations were attributed to excessive sensor gradients and replaced by an arbitrary value of +500 nT/m. These flag values are evident as pink-coloured rectangular signatures. Although the true amplitude and polarity of the vertical magnetic gradient at these locations is unknown, it may be possible to infer the actual polarity from surrounding values.

Note that, in general, isolated extreme data values can give rise to apparently rectangular signatures, as a result image discretization effects, and due caution is warranted in connection with related interpretation.

For all Phase II magnetic investigations, vertical gradient readings were acquired at 0.5 m intervals along east-west transects separated by 0.5 m. As for conductivity surveys, data acquisition was initiated from the local southeast grid corner.

Measurements and associated grid coordinates were digitally recorded via integrated memory and subsequently downloaded to a portable field computer for processing and analysis.

2.3 Ground Penetrating Radar

Phase II radar investigations were carried out using a GSSI SIR-2000 digital radar system with 400 MHz transceiver. Continuous radar soundings were acquired by towing the active antenna package at an approximately constant rate along specified transects with location constrained by fiducial marks, recorded digitally in conjunction with data acquisition.

In connection with focused electromagnetic conductivity and magnetic gradient surveys of HP11, HP20 and HP24, GPR scans were acquired on coincident east-west transects at 0.5 m interval and with fiducial marks recorded at 0.5 m intervals along profile. In all cases, radar acquisition was initiated at the corresponding northeast grid corner. Resulting data vectors were subsequently resampled within specified time windows to compute plans of mean reflectivity for comparison with corresponding conductivity and gradient magnetic distributions. The resampling process is illustrated in Figure 8.

In contrast with conductivity and magnetic mapping methods, coincident ground radar coverage yields a three dimensional data volume that can be subsequently resampled on specified planes to yield both vertical cross-sections as well as well as plan-sections at arbitrary time or depth horizons. There is clearly substantial flexibility in specifying related parameters and extensive experimentation indicates that for preliminary assessment and comparison with coincident conductivity and magnetic results, a relatively coarse resampling is advantageous. In particular, for initial results presented herein, horizontal cell dimensions were taken equal the nominal grid interval of 0.5 m. In other words, with reference to Figure 8, spatial averaging is restricted to a single radar scan ($\delta x = \Delta x = 0.5$ m) with window length

equal to the fiducial interval ($\delta y = \Delta y = 0.5$ m). Given a total recorded two-way transit time of $\Delta t = 40$ ns, the corresponding time window is taken as $\delta t = \Delta t / 3 = 13.33$ ns. In particular, assuming an effective radar velocity of approximately $v = 0.15$ m/ns (estimated from data), $\delta t = 13.33$ ns yields effective depth windows of 0 – 1 m, 1 – 2 m and 2 – 3 m below local grade (no correction has been made for topography).

Radar reflectivity plans have been computed for both raw and absolute amplitudes and it is noted that corresponding results display significantly different and complementary character. In all cases, an averaged background reflectivity has been subtracted from raw soundings to remove the influence of transient inductive effects and system-generated noise. Finally, to emphasize larger scale features, resulting images have been spatially filtered by application of a 9-point (3 x 3) Hanning operator to further smooth resampled data.

It is emphasized that there is much that can be done with the existing GPR data beyond the coarse scale plans presented herein. In connection with future archaeological interpretation, specific features or horizons can be investigated in greater detail, in cross-section and/or plan-view, by specifying appropriately refined resampling parameters. It is also possible to specify a local time/elevation reference surface (default is local surface elevation) to yield plans of radar reflectivity bracketing particular stratigraphic horizons or cultural levels.

3.0 RESULTS

3.1 HP24 / HP36

Plans displaying measured apparent electrical conductivity and vertical magnetic gradient are presented in Figure 9. Indicated colour levels are based on interpolations and extrapolations from discrete measurements on 0.5 m x 0.5 m centers.

As expected, results are generally consistent with preliminary site-wide surveys. However, increased acquisition density has yielded substantially improved detection and resolution of smaller-scale house-floor features. Although meaningful and confident interpretation of these features requires subsequent comparison and correlation with available archaeological data, observed spatial distribution and patterning of geophysical signatures suggests that these features are potentially significant. For example, it is unlikely that the symmetric pattern of gradient magnetic signatures at the center of HP36 is of natural origin.

In general, there appears to be close correspondence between localized house-floor features as tentatively indicated by magnetic and conductivity surveys. On a larger scale, the conductivity plan suggests that HP24 is characterized by a relatively rectangular floor area compared with HP36. In addition, it is noted that there is indication of a number of significant and localized features within rim deposits at the northeast of HP36.

There is also some indication of potential internal structure within the large external pit feature, located south of HP24 and west of HP36. However, the strong and largely continuous magnetic gradient signature suggests that this feature is a roasting pit or other fire-related activity feature.

Figures 10-13 display corresponding ground radar reflectivity plans for HP24 together with the corresponding magnetic gradient plan for comparative reference. Indicated colour levels are based on interpolations and extrapolations from resampled reflectivity data at 0.5 m x 0.5 m cell centers. In particular, Figures 10 and 12 display averaged raw reflectivity levels for interpreted depth ranges of 0 – 1 m and 1 – 2 m, respectively. Figures 11 and 13 display corresponding plans of averaged absolute reflectivity for the same interpreted depth ranges.

In general, despite resampling and related averaging, it is observed that GPR plans display higher frequency variability than corresponding results for electrical conductivity and magnetic gradient. Nonetheless, significant correspondence is observed between certain GPR reflectivity signatures and related conductivity and magnetic features. For HP24, this correspondence is substantially greater for the 1 – 2 m depth range (Figures 11 and 13) than for the associated near-surface distributions (Figures 10 and 12), indicating that principal house-floor features are largely located within the 1 – 2 m range. Moreover, results for a deeper 2 – 3 m interval displayed comparatively little coherent signal, suggesting that cultural deposits do not extend substantially beyond the 2 m level.

Again, meaningful and confident interpretation of GPR signatures requires subsequent comparison and correlation with available archaeological information.

3.2 HP20

Figure 14 displays apparent electrical conductivity and vertical magnetic gradient as measured for HP20 and surrounding area. As for HP24/HP36, indicated

colour levels are based on interpolations and extrapolations from discrete measurements at 0.5 m x 0.5 m grid nodes. Again, enhanced resolution has revealed a well-defined and potentially significant spatial distribution of small-scale geophysical signatures within the house-floor area. Moreover, there is also, again, good correlation between anomalous magnetic and conductivity features.

In addition, conductivity and particularly magnetic plans display evident, well-defined signatures in connection with numerous external pit features, located within rim deposits and otherwise surrounding HP20.

Corresponding GPR reflectivity plans, focused on HP20, are presented in Figures 15–18, together with the associated gradient magnetic plan for reference. As for the previous case, indicated colour levels are based on interpolations and extrapolations from resampled reflectivity data at 0.5 m x 0.5 m cell centers. Figures 15 and 17 display averaged raw reflectivity levels for interpreted depth ranges of 0 – 1 m and 1 – 2 m, respectively. While, Figures 16 and 18 display corresponding plans of averaged absolute reflectivity for the same interpreted depth ranges.

Once again, although resulting GPR reflectivity plans display relatively high-frequency variability compared with associated magnetic and conductivity plans, gross correlation is observed between certain larger-scale signatures. For instance, all plans display a concentration of anomalous signatures in the area bounded by 0W-5W and 95N-100N. In general, correlation between GPR, magnetic and conductivity distributions is greater for the 1 – 2 m radar depth interval (Figures 16 and 18) than for the shallower interval (Figures 15 and 17). However, compared with results for HP24/HP36, there appears to be substantially better correlation for the 0 – 1 m interval, suggesting that related subsurface features are somewhat shallower at HP20.

Again, the archaeological significance or interpretation of specific GPR signatures is beyond the scope of the present report.

3.3 HP11 / HP10

Measured apparent electrical conductivity and vertical magnetic gradient for HP11 / HP10 are displayed in Figure 19. Indicated colour levels are, again, based on interpolations and extrapolations from discrete measurements on 0.5 m x 0.5 m centers. Phase II results are generally consistent with preliminary site-

wide surveys. However, extended resolution provides enhanced discrimination of numerous, and patterned, small-scale features both within and external to house-floor areas.

HP11 is unusual in that a well-defined bench deposit exists interior to and concentric with the pit-house rim and appears to be contemporaneous with a narrow breach of the rim on the northwest at approximately 33E, 55N. These features are clearly delineated by conductivity and gradient magnetic surveys displayed in Figure 19. In particular, while rim deposits are delineated by anomalous magnetic gradients, interior and concentric bench deposits are clearly indicated by anomalously elevated conductivity levels. Moreover, it is noted that elevated conductivity levels extend through the identified breach on the northwest rim. In addition, although there is a tendency for topographic lows to be associated with elevated moisture levels and anomalously higher electrical conductivities, the conductivity of bench deposits exceeds that of the interior house-floor area at lower elevation. Conductivity results also suggest generally and substantially different material conditions within HP11 and HP10 house floors.

Corresponding radar reflectivity plans for HP11 are displayed together with the associated gradient magnetic plan in Figure 20–23. Again, indicated colour levels are based on interpolations and extrapolations from resampled reflectivity data at 0.5 m x 0.5 m cell centers. Figures 20 and 22 display averaged raw reflectivity levels for interpreted depth ranges of 0 – 1 m and 1 – 2 m, respectively. While, Figures 21 and 23 display corresponding plans of averaged absolute reflectivity for the same interpreted depth ranges.

In contrast with previous cases, it is noted that absolute reflectivity distributions appear to display a generally better correlation with the results of magnetic and conductivity surveys. Moreover, the correlation is substantially better for the near-surface (0 – 1 m) depth interval, suggesting that potential cultural features are relatively shallow.

Again, GPR plans display substantially greater small-scale variability and apparent detail than corresponding conductivity or gradient magnetic maps. However, the extent to which this apparent detail is interpretable and meaningful requires further investigation in connection with subsequent archaeological excavations. Larger-scale patterning displays good correlation with related magnetic and conductivity features and provides supporting and complementary information to clarify and extend the interpretation of these data.

3.4 HP54

Prior to conducting high-density, grid-based reconnaissance described in previous sections, limited ground radar investigations were undertaken in HP54 to assess the nature and potential continuity of stratified deposits encountered by preliminary excavations. Stratigraphy in test unit 175N, 21W included roof and rim zones within the upper 0.5 m, overlying a thick sequence of floor-like deposits (approximately 1.30 m) with about 5 hearth features and a cache pit (Prentiss, personal communication).

To investigate whether these deposits might extend laterally as a consistently thick floor with varying feature frequencies, a series of GPR scans were acquired through and adjacent to the Test unit at 175N, 21W. In particular, a west-east GPR scan was acquired parallel to and approximately 0.5 m north of the 175N gridline, between 24W and 8W, with three orthogonal scans at approximately 19.5W, 18.5W and 17.5W.

Figure 24 displays the west-east scan acquired at roughly 175.5N and intersecting the 2004 excavation unit at approximately 21W. The near-surface expression of the excavation is clear and, as indicated in the exploded view, the excavation appears to have penetrated the center and vertical extent of a broader anomalous feature associated with the deposit. The scan indicates two other localized, albeit lesser, features along the 175.5N transect and orthogonal south-north scans at 19.5W and 17.5W give (Figure 25) clear indication of additional interesting features within the central area of the house floor. As noted (Figure 24), two-way transit time to the interpreted base of the 2004 excavation unit, implies an effective radar velocity of roughly $v=0.15$ m/ns, consistent with data-based estimation.

In general, GPR scans indicate that the excavated feature is anomalous both in terms of radar reflectivity and apparent thickness. Results suggest that surrounding stratified floor deposits are semi-continuous and of fairly consistent thickness (approximately 1.0 m on average), however, substantially thinner than the excavated feature deposit. It is anticipated that additional anomalous and localized GPR features are attributable to similar feature concentrations. However, it is noted that the extent and character of these anomalous reflectivity zones varies significantly, suggesting considerable variability in the nature and composition of associated deposits.

In particular, the excavated feature was initially identified on the basis of its anomalous magnetic response and, consequently, it is anticipated that other GPR features with comparable magnetic signatures might be due to similar stratified hearth deposits. In contrast, additional anomalous reflectivity features,

without corresponding magnetic signatures but, potentially, with abnormal electrical conductivity levels, might be due to concentrations of rock or non-fire related pit features. In general, correlation and comparison of complementary geophysical signatures can substantially constrain and guide appropriate interpretation.

Unfortunately, in the case of HP54, preliminary site-wide coverage does not provide sufficient resolution to address the nature of smaller-scale features. However, results presented in previous sections suggest that this is precisely the sort of interpretive potential afforded by Phase II data. In addition, while preliminary Phase II radar results reported in Sections 3.1–3.3 are presented in plan-view format, results for HP54, displayed in Figures 24 and 25 demonstrate the complementary nature of a cross-sectional display format.

4.0 CONCLUDING REMARKS

Within the site-wide context provided by preliminary surveys presented in Figures 2 and 3, Phase II geophysical investigations have provided a detailed focus on selected pit houses and related external features. Coincident, high-density EM conductivity, magnetic gradient and radar reflectivity surveys have mapped numerous well-defined and correlated geophysical signatures that are potentially indicative of related archaeological deposits.

No attempt has been made herein to infer or interpret the archaeological significance of recorded geophysical signatures. Meaningful interpretation requires subsequent integrated and cooperative analysis and assessment of geophysical findings in connection with related archaeological data and relevant contextual information.

Phase II acquisition density was nominally 0.5 m x 0.5 m providing a reasonable tradeoff between coverage and resolution. Ground radar scans provide substantially higher resolution (<0.05 m) along transect. Although it was originally proposed to restrict Phase II investigations to pit-house floor areas, it was decided to extend higher-definition coverage to include surrounding rim deposits and sufficient background to provide adequate spatial context for analysis and interpretation. On the basis of results presented here, it is apparent that current resolution provides sufficient detail for recognition and identification of features on the scale of archaeological interest. Moreover, as required, existing data can be re-processed and/or filtered to extract additional information and to provide further constraints on interpretation.

Finally, as warranted, Phase II results can be augmented by yet higher density focused surveys to further investigate the nature of specific features. In Particular, substantially higher-resolution ground radar images can be acquired by employing a higher frequency transducer and reducing the transect interval. In addition, it is anticipated that resolution of electrical conductivity images can be substantially improved via small-scale pole-pole, probe resistivity measurements.

Ultimately, it is envisioned that substantial portions of Phase II investigated areas will be excavated to validate the findings of geophysical reconnaissance. In general, the interpretive potential of geophysical data increases dramatically as archaeological investigations establish a direct correspondence between geophysical signatures and related archaeological deposits. It is anticipated that confirmation of consistent and repeatable associations between common archaeological features and their geophysical signatures would facilitate an efficient extension of archaeological findings to other areas of the site with reduced necessity for excavations.

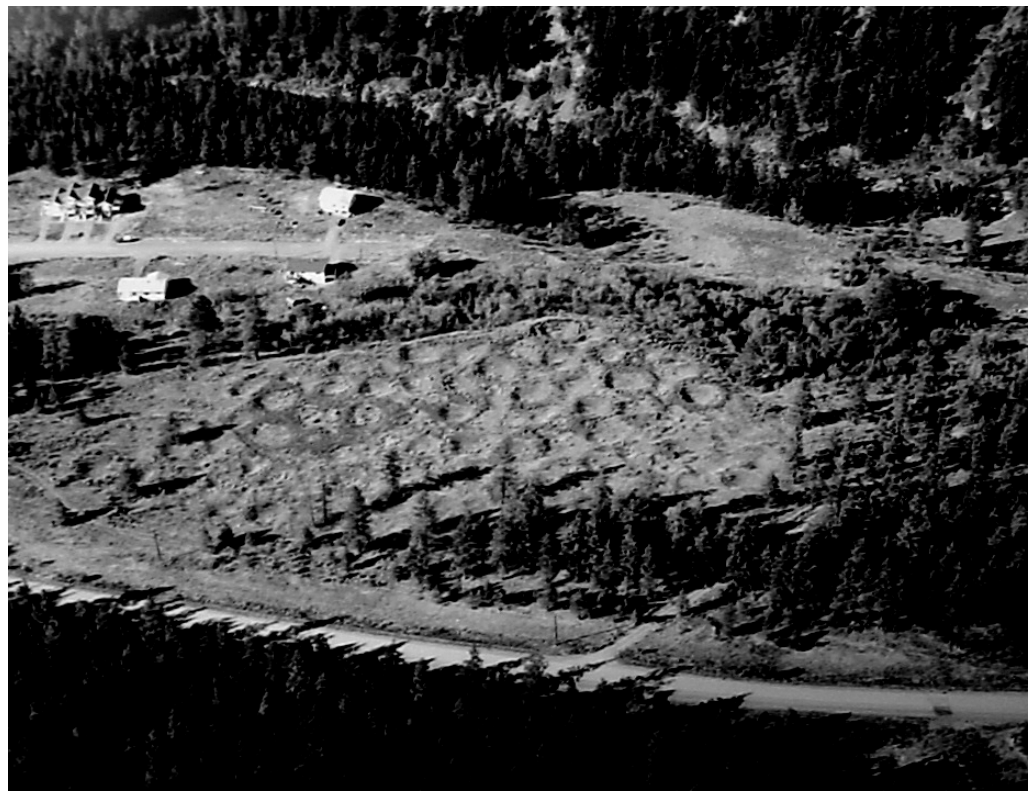
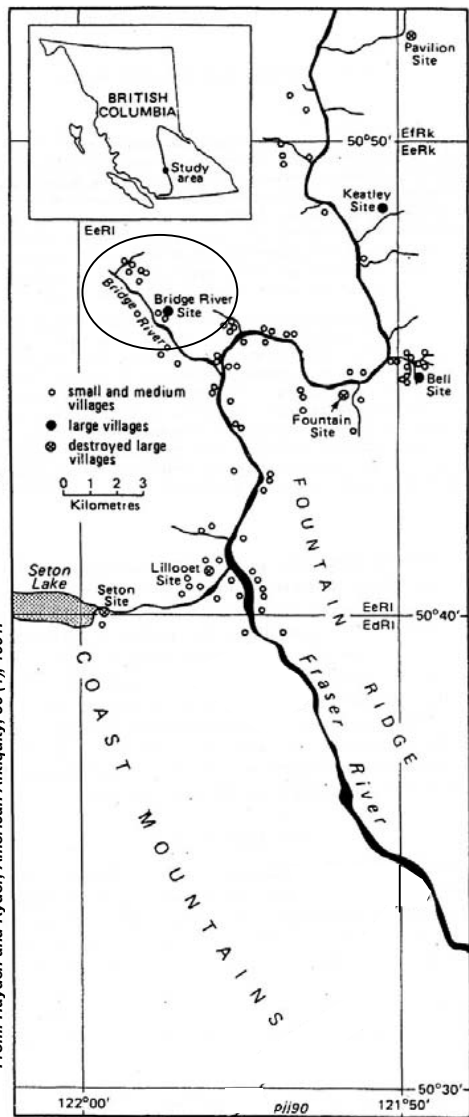
We trust that this report of Phase-II geophysical investigations satisfies your current requirements and look forward to a cooperative effort on subsequent archaeological interpretation. Should you require additional information or clarification regarding activities or findings presented herein, please contact the undersigned at your convenience.

Yours truly,
Terrascan Geophysics

Guy Cross, Ph.D.
Geophysicist

5.0 REFERENCE

Cross, G. M., 2004, Bridge River archaeological project – geophysical investigations, Phase I – Final Report, Department of Anthropology, University of Montana, Missoula.



**BRIDGE RIVER SITE (EeRI-4)
LOCATION PLAN – AERIAL SITE PHOTO**

FIGURE:

1

PROJECT:

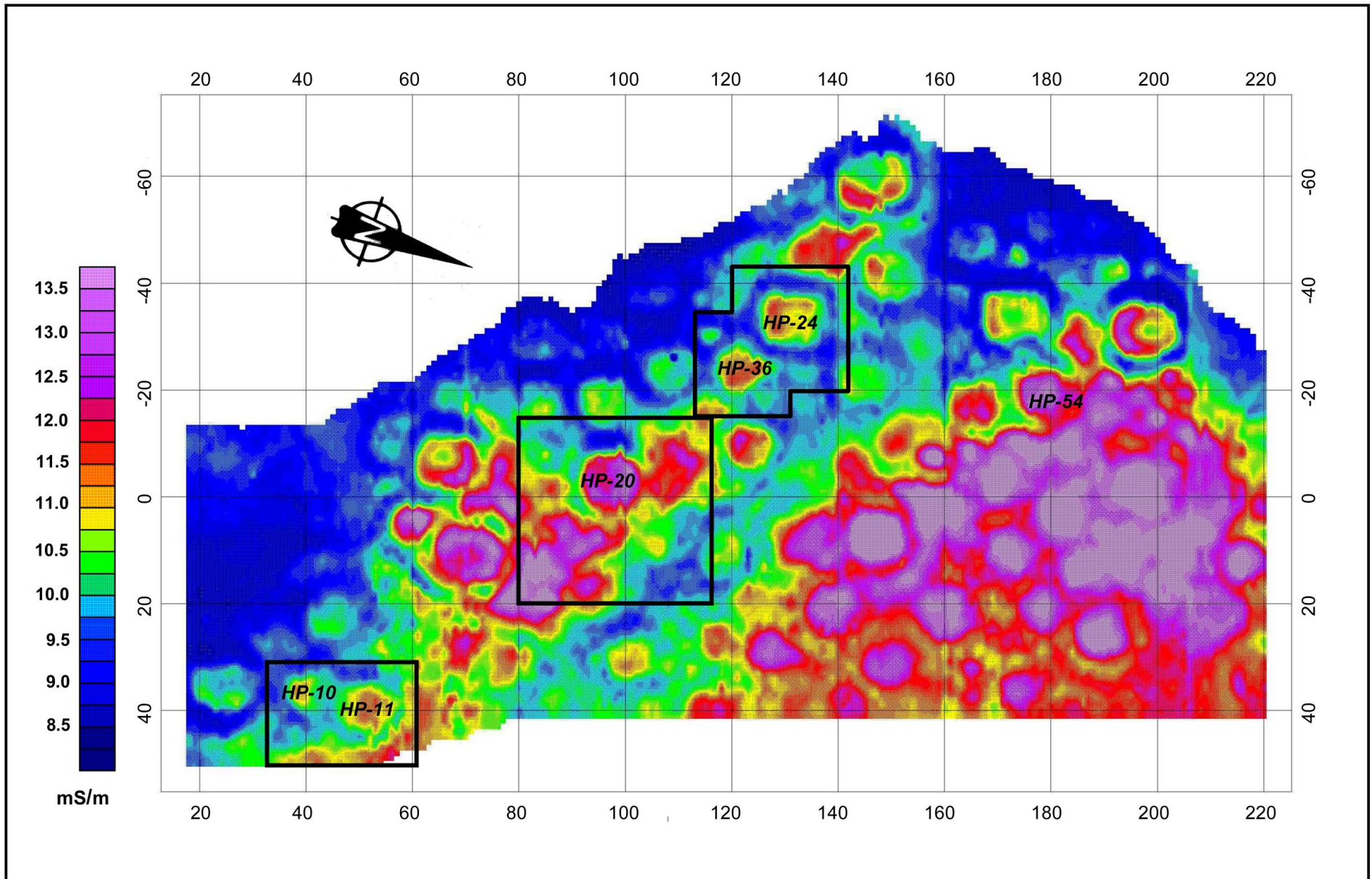
Univ. Montana – Bridge River

DRAWN BY:

GMC

DATE:

15 July, 2005



**BRIDGE RIVER SITE (EeRI-4) – APPARENT CONDUCTIVITY
PHASE II INVESTIGATION AREAS**

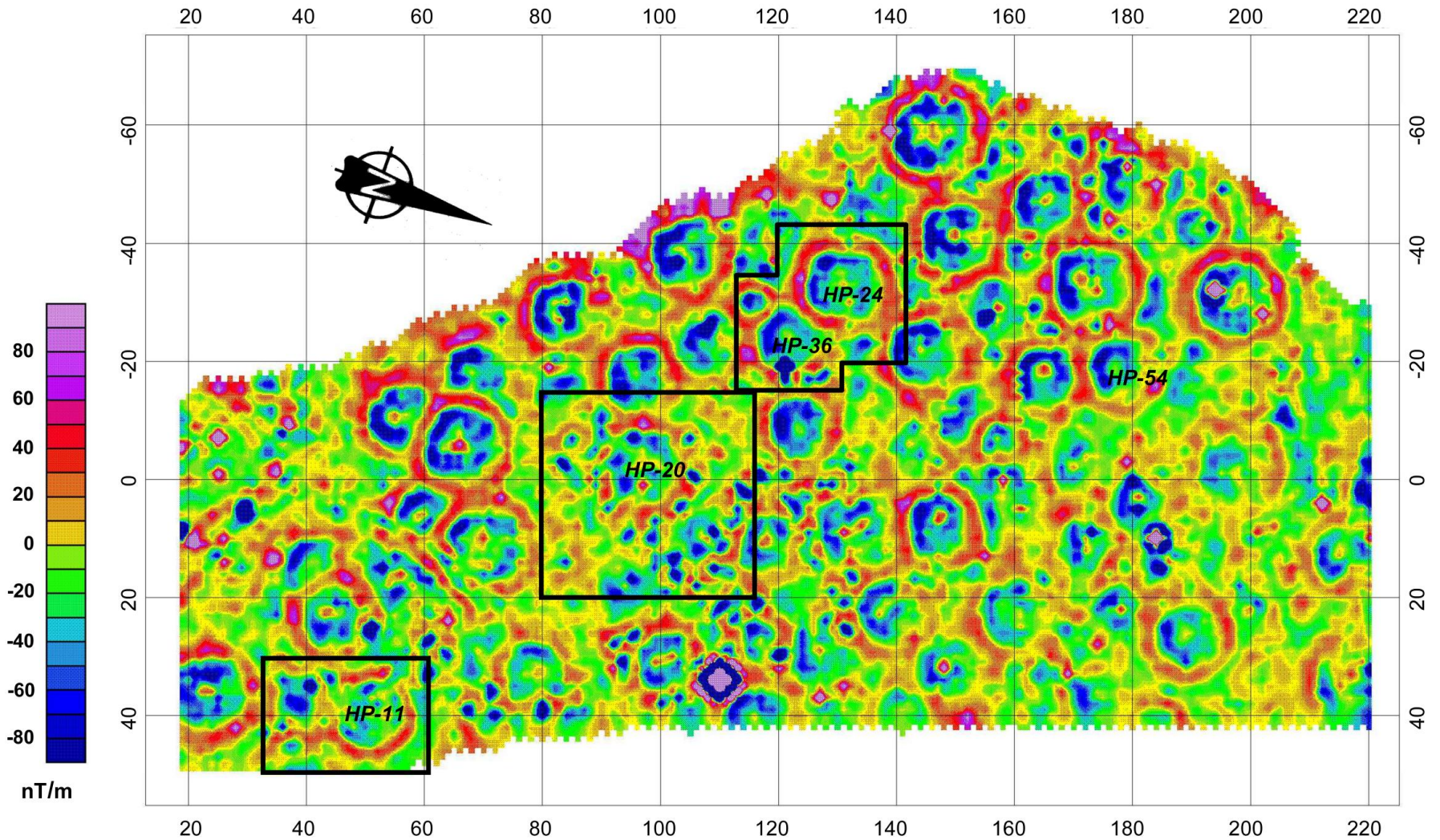
FIGURE:

2

PROJECT: *Univ. Montana – Bridge River*

DRAWN BY: *GMC*

DATE: *28 July, 2003*



**BRIDGE RIVER SITE (EeRI-4) – MAGNETIC GRADIENT
PHASE II INVESTIGATION AREAS**

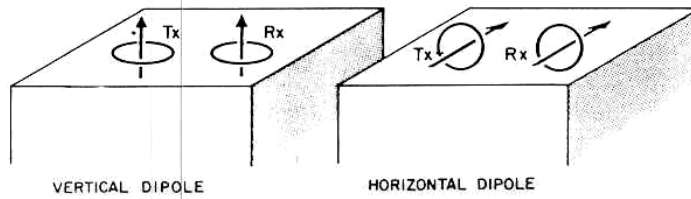
FIGURE:

3

PROJECT: *Univ. Montana – Bridge River*

DRAWN BY: *GMC*

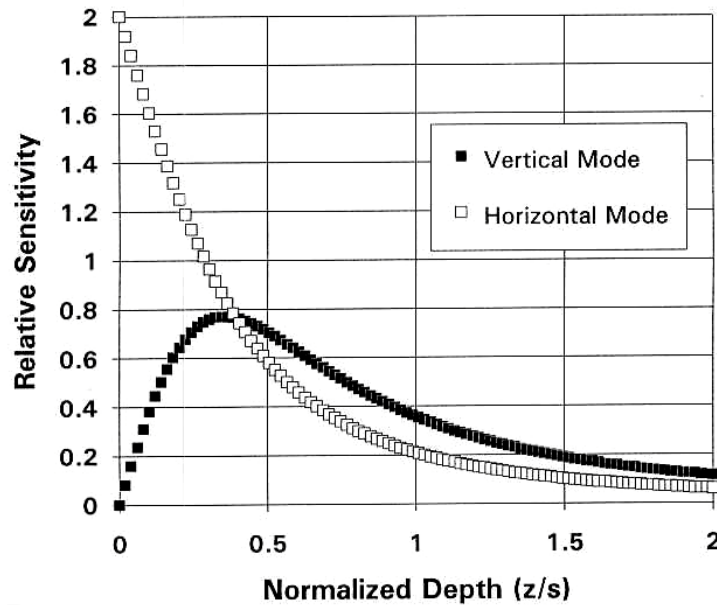
DATE: *27 December, 2003*



Instrument	Intercoil Separation (m)	Peak Sensitivity (m)		Effective Range (m)	
		Horizontal (z=0.0)	Vertical (z=0.35s)	Horizontal (z=0.75s)	Vertical (z=1.5s)
EM-38	s=1.0	0.0	0.35	0.75	1.5
EM-31	s=3.7	0.0	1.3	2.8	5.6
EM-34	s=10.0	0.0	3.5	7.5	15.0
	s=20.0	0.0	7.0	15.0	30.0
	s=40.0	0.0	14.0	30.0	60.0

NOTE: Effective range refers to 70% cumulative response.

Normalized Depth Sensitivity



GEONICS EM-38 / EM-31 / EM-34 - RESPONSE CHARACTERISTICS



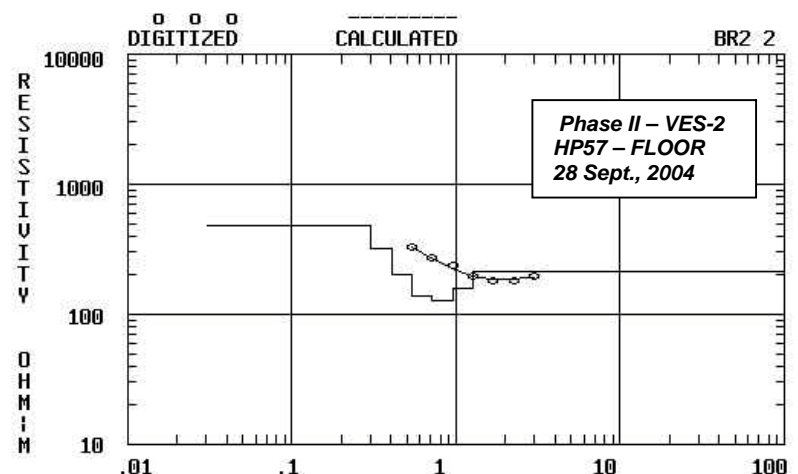
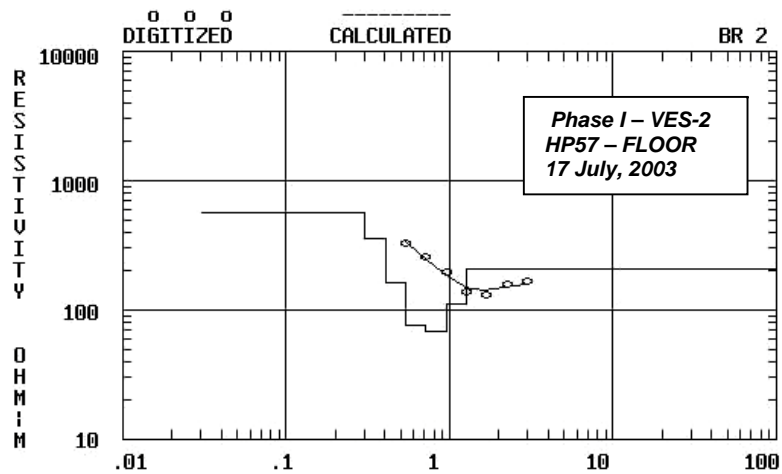
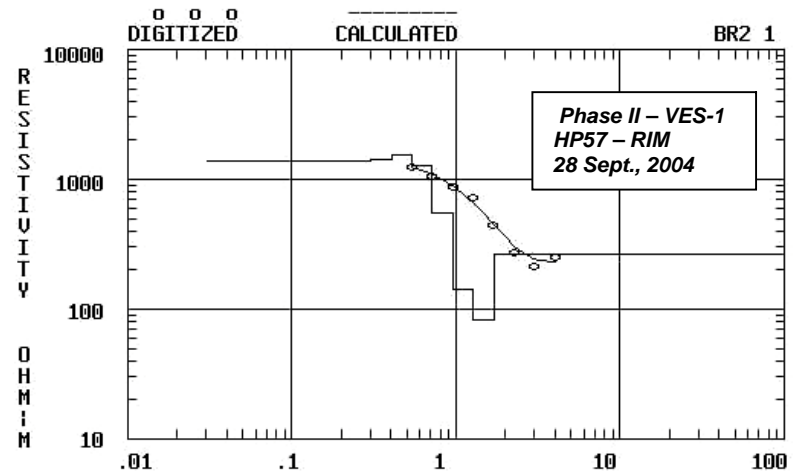
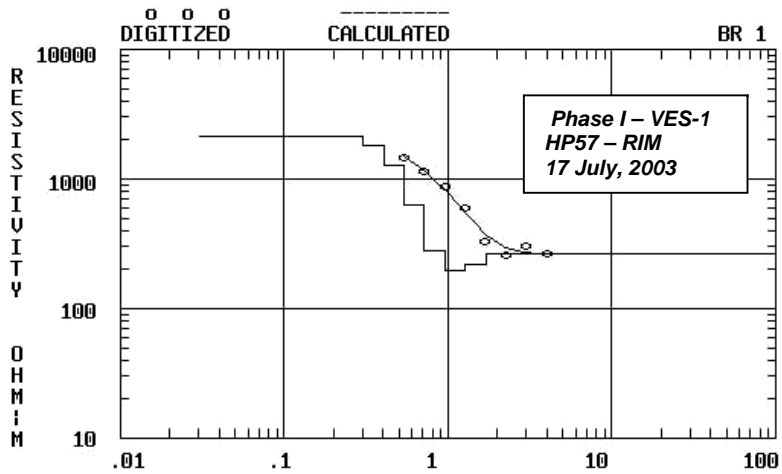
PROJECT: Univ. Montana – Bridge River

FIGURE:

DRAWN BY: GMC

DATE: 14 October, 2003

4



ELECTRODE SPACING (a), OR DEPTH, IN METERS

ELECTRODE SPACING (a), OR DEPTH, IN METERS



**BRIDGE RIVER SITE (EeRI-4) - HP57
VERTICAL ELECTRICAL SOUNDINGS - WENNER CONFIGURATION
INVERTED RESISTIVITY - DEPTH STRUCTURES**

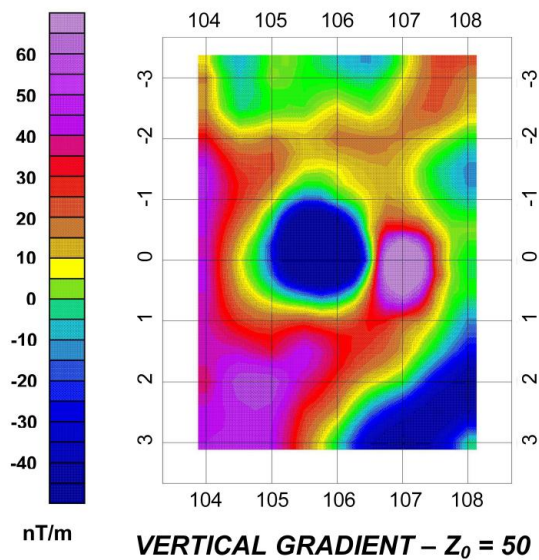
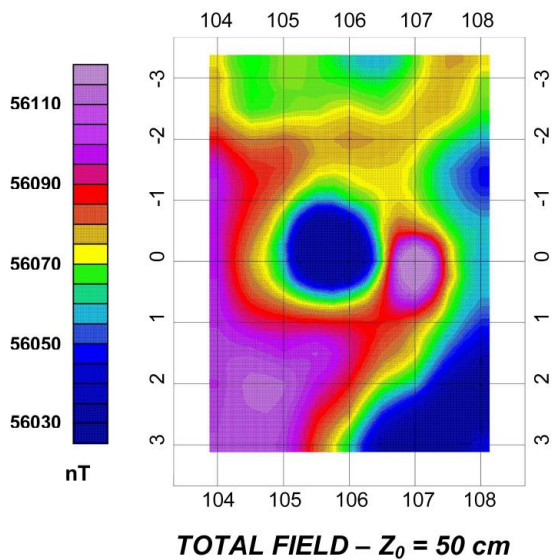
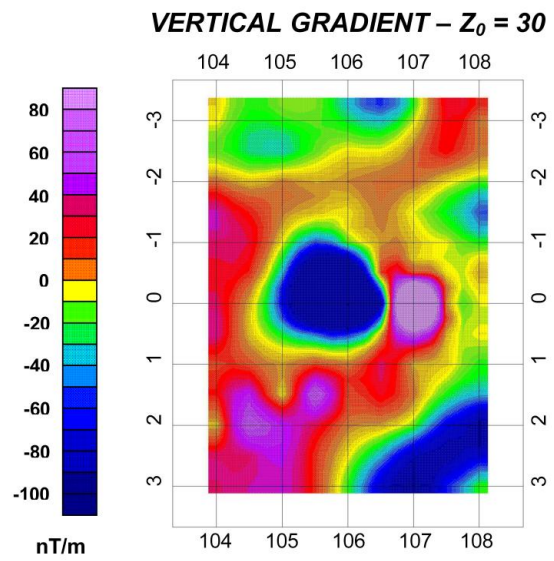
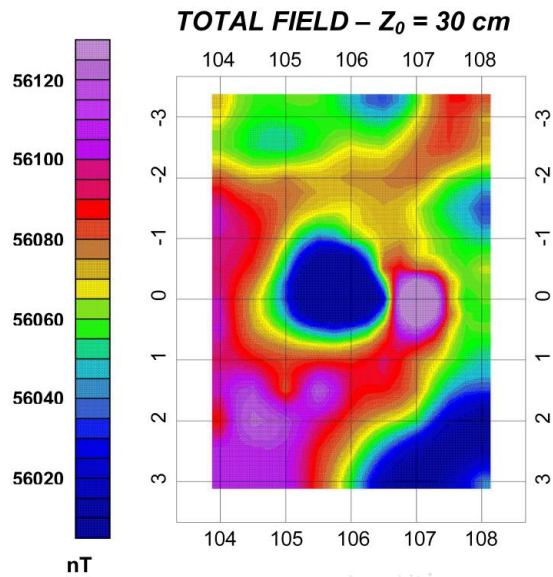
FIGURE:

5

PROJECT: Univ. Montana - Bridge River

DRAWN BY: GMC

DATE: 13 October, 2004



**BRIDGE RIVER SITE (EeRI-4) – EPF MAGNETIC SIGNATURE (0E,106N)
TOTAL FIELD / VERTICAL GRADIENT / SENSOR HEIGHT**



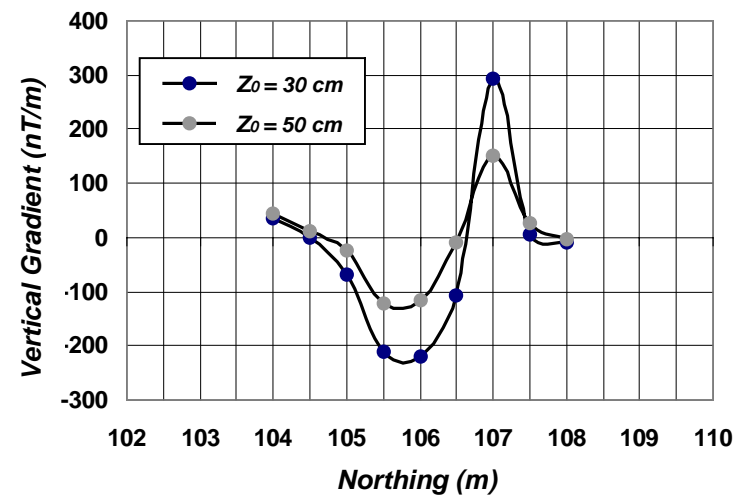
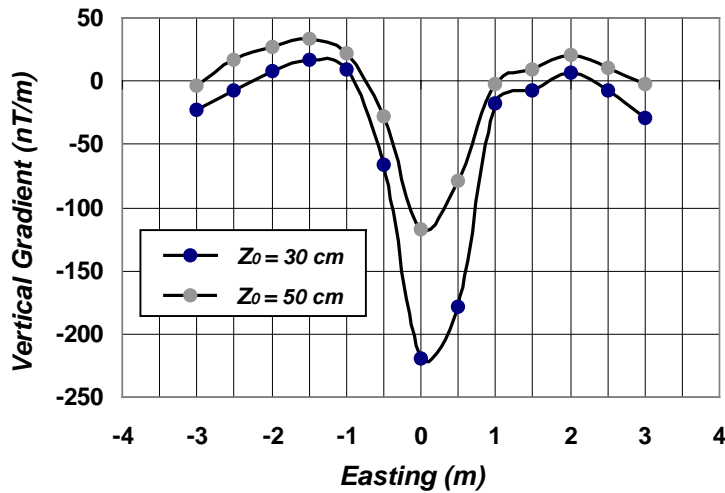
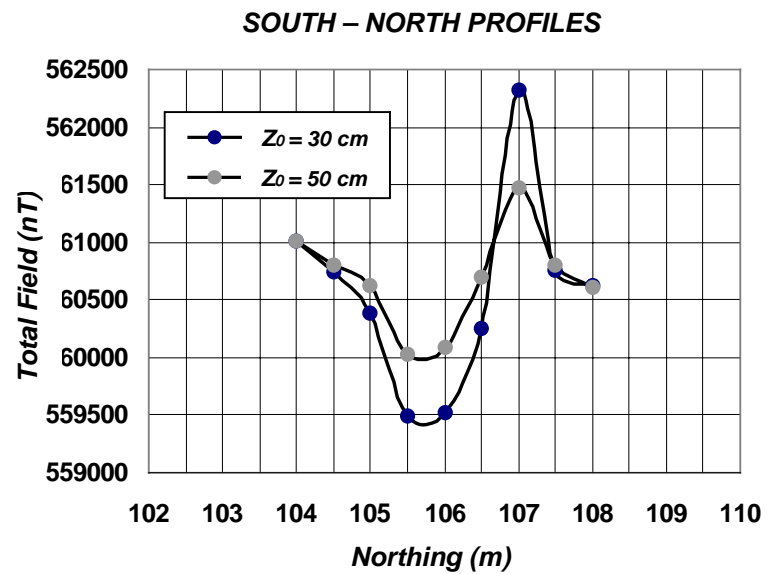
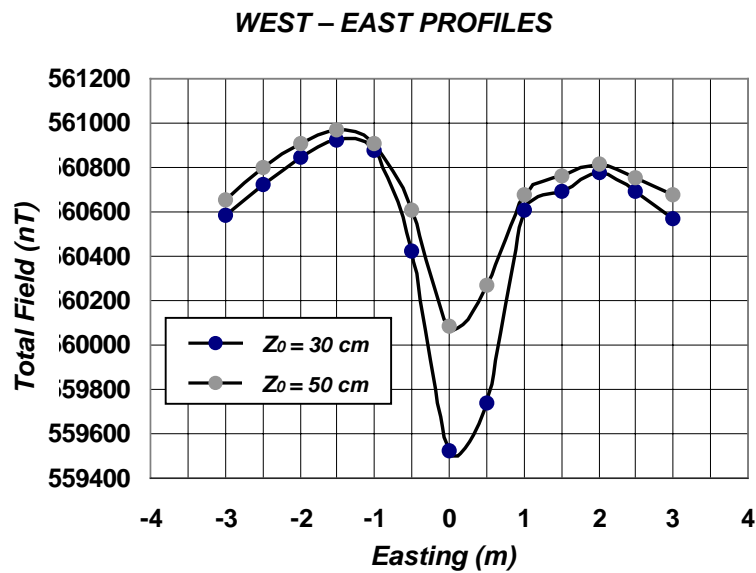
PROJECT: *Univ. Montana – Bridge River*

FIGURE:

DRAWN BY: *GMC*

DATE: *30 October, 2004*

6



**BRIDGE RIVER SITE (EeRI-4) – EPF (0E,106N)
TOTAL MAGNETIC FIELD – VERTICAL GRADIENT PROFILES**

FIGURE:

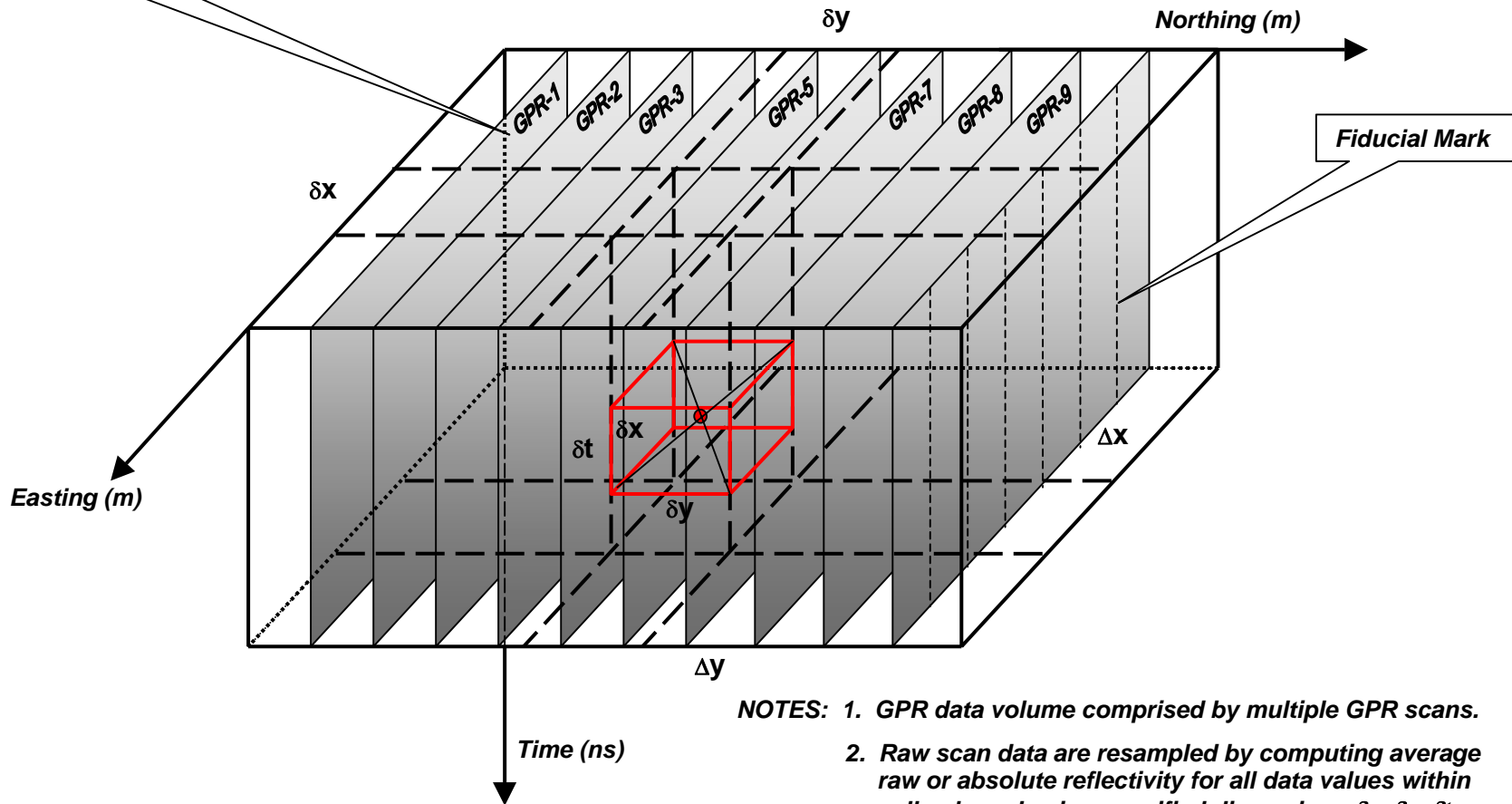
7

PROJECT: Univ. Montana – Bridge River

DRAWN BY: GMC

DATE: 10 October, 2004

Raw GPR Scan



- NOTES: 1. GPR data volume comprised by multiple GPR scans.
2. Raw scan data are resampled by computing average raw or absolute reflectivity for all data values within cell volume having specified dimensions δx , δy , δt . Computed mean value is assigned to cell midpoint.
3. Δy and Δx denote scan and fiducial intervals.



**GROUND PENETRATING RADAR
DATA VOLUME RESAMPLING PROCESS**

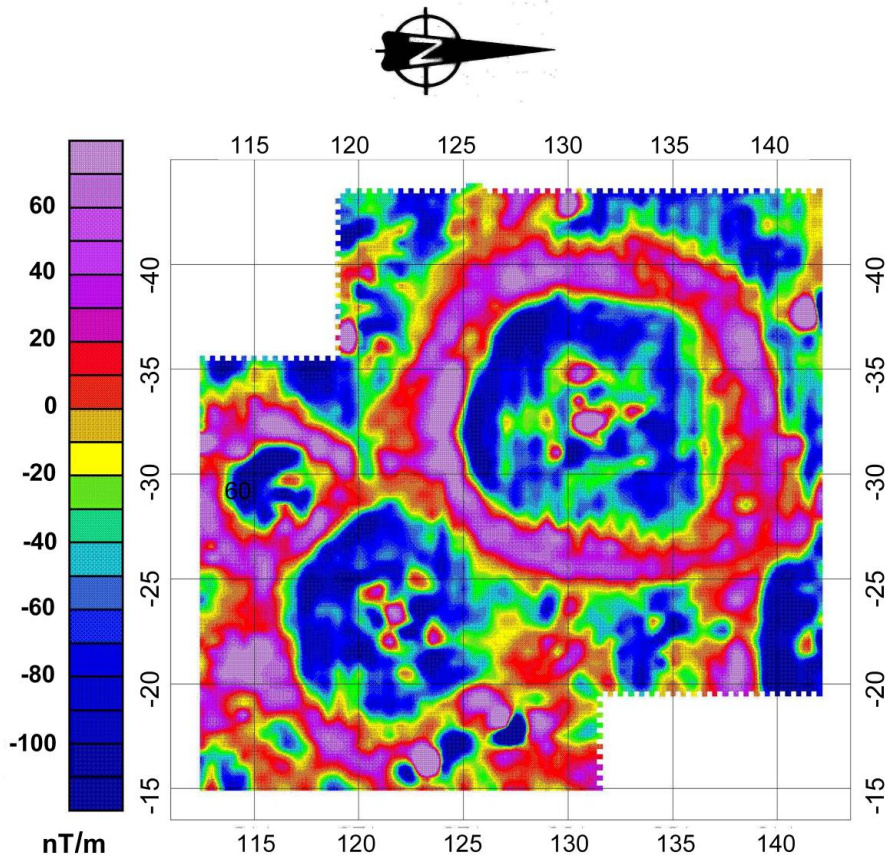
FIGURE:

8

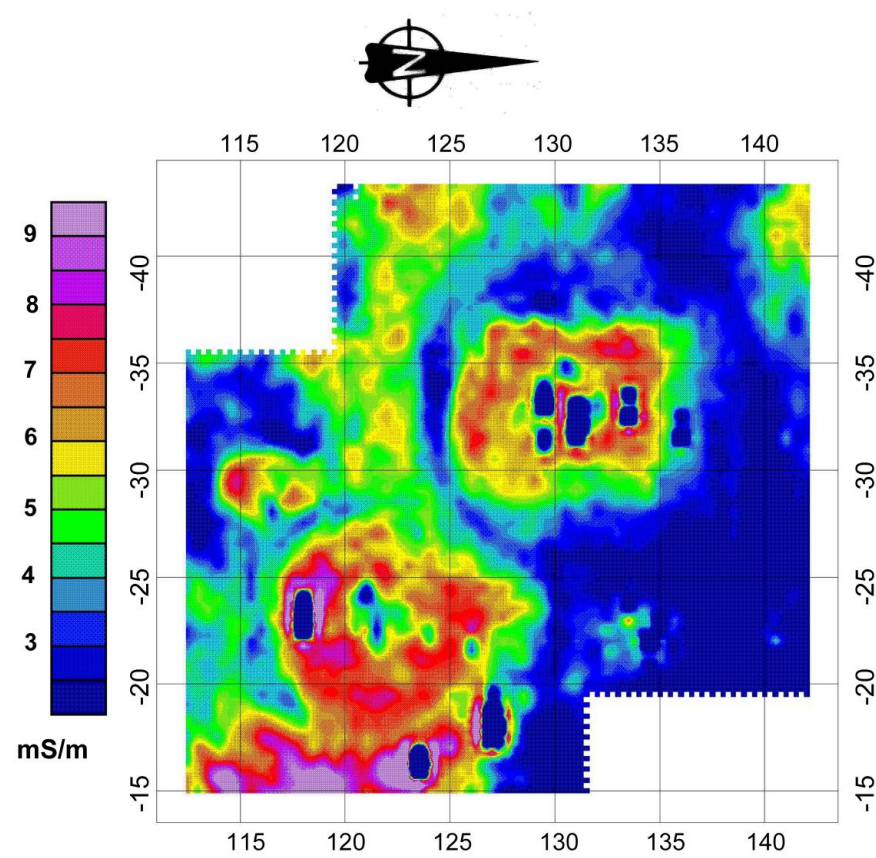
PROJECT: Univ. Montana – Bridge River

DRAWN BY: GMC

DATE: 5 July, 2005



VERTICAL MAGNETIC GRADIENT



APPARENT ELECTRICAL CONDUCTIVITY

NOTE: Colour scale distributions are approximate and based on interpolation-extrapolation from discrete data.



**BRIDGE RIVER SITE (EeRI-4) – PIT HOUSES 24 / 36
VERTICAL MAGNETIC GRADIENT – APPARENT CONDUCTIVITY**

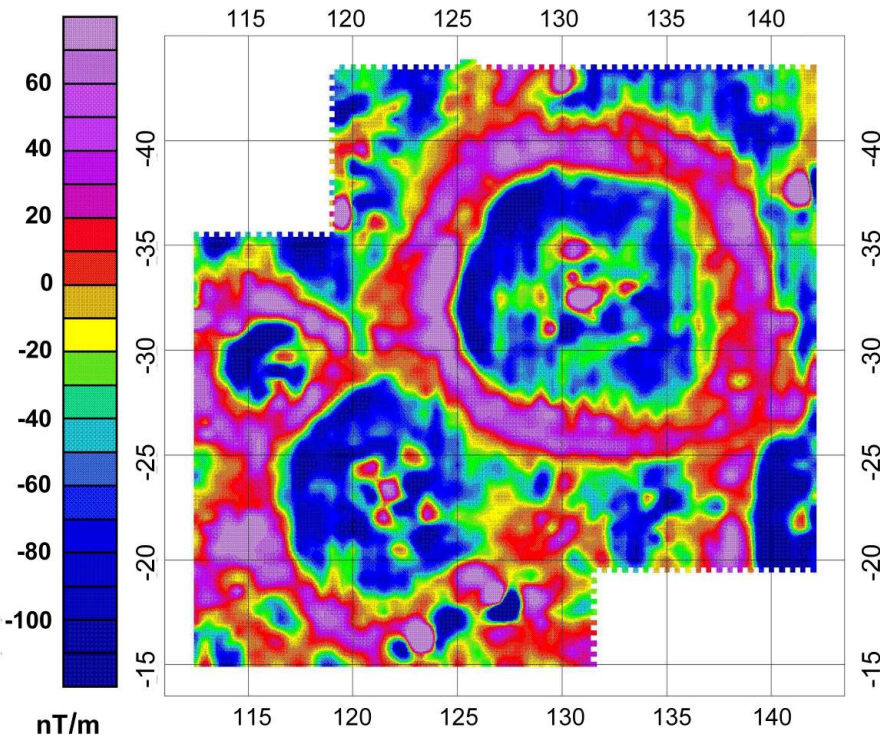
FIGURE:

9

PROJECT: *Univ. Montana – Bridge River*

DRAWN BY: *GMC*

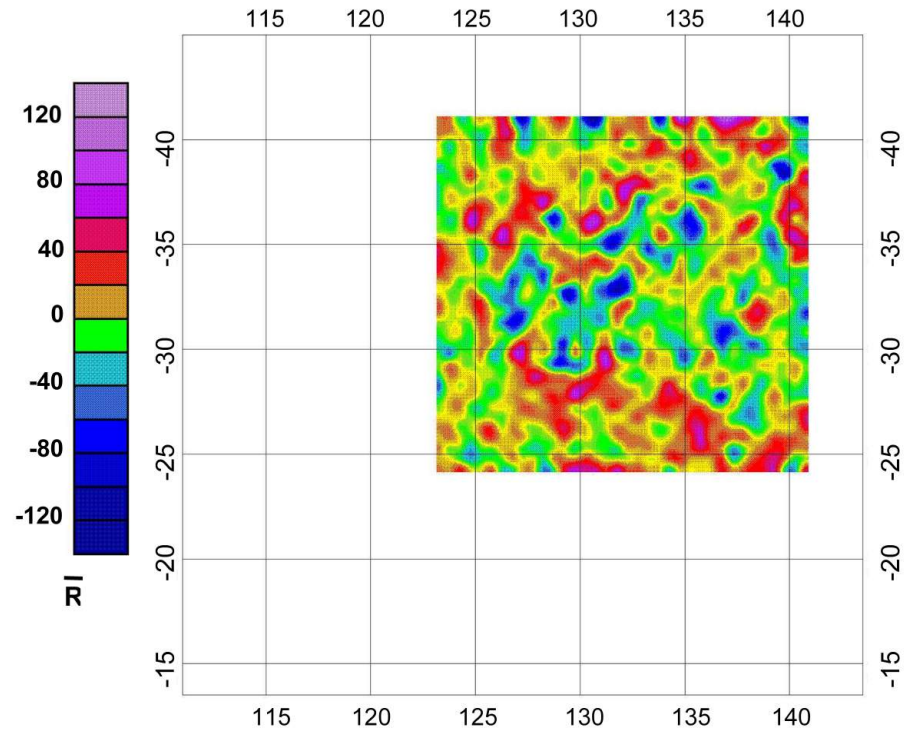
DATE: *12 October, 2004*



VERTICAL MAGNETIC GRADIENT

NOTE: Colour scale distributions are approximate and based on interpolation-extrapolation from discrete and time-sampled (GPR) data.

Indicated radar depth levels based on interpreted velocity $v=0.15$ m/ns via diffraction-based velocity estimation.



GROUND RADAR RAW REFLECTIVITY

Raw Reflectivity 0.0 – 13.3 ns (~0.0 – 1.0 m)
 $\Delta x=0.5$ $\Delta y=0.5$
 3x3 Hanning filter (x1)



BRIDGE RIVER SITE (EeRI-4) – PIT HOUSES 24 / 36
VERTICAL MAGNETIC GRADIENT – RADAR REFLECTIVITY
RAW REFLECTIVITY – ZERO MEAN – 0.0-1.0 m

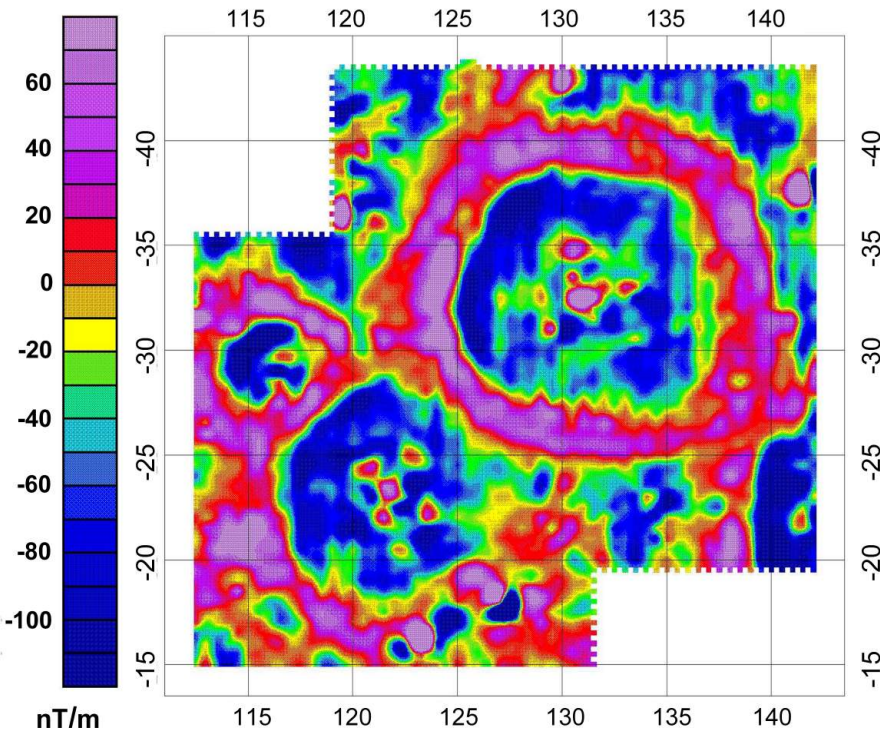
FIGURE:

10

PROJECT: Univ. Montana – Bridge River

DRAWN BY: GMC

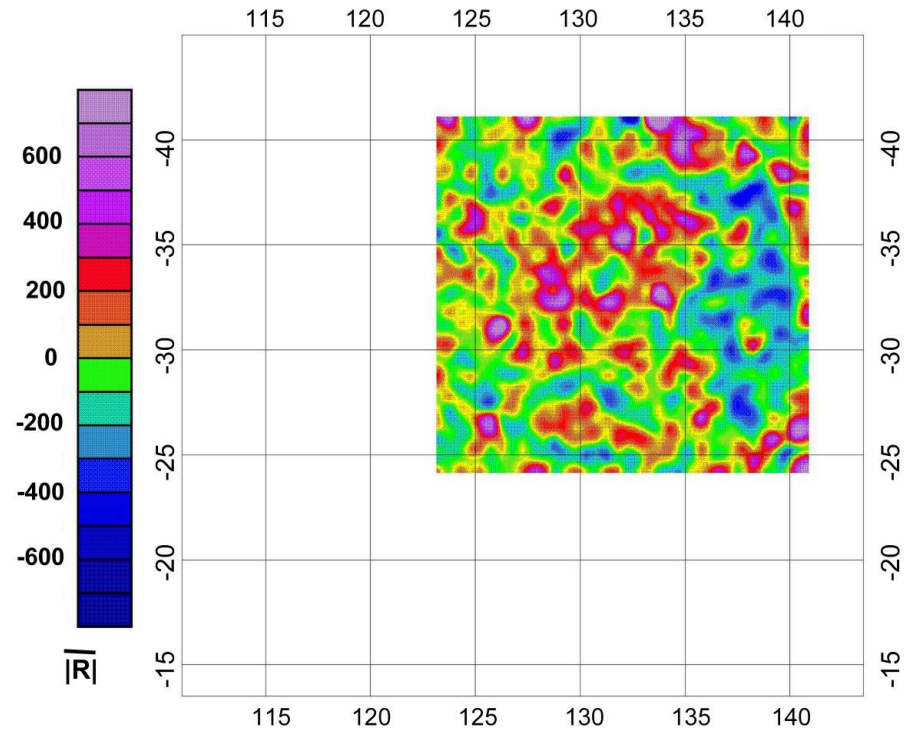
DATE: 27 June, 2005



VERTICAL MAGNETIC GRADIENT

NOTE: Colour scale distributions are approximate and based on interpolation-extrapolation from discrete and time-sampled (GPR) data.

Indicated radar depth levels based on interpreted velocity $v=0.15$ m/ns via diffraction-based velocity estimation.



GROUND RADAR REFLECTIVITY

Absolute Reflectivity 0.0 – 13.3 ns (~0.0 – 1.0 m)
 $\Delta x=0.5$ $\Delta y=0.5$
 3x3 Hanning filter (x1)



BRIDGE RIVER SITE (EeRI-4) – PIT HOUSES 24 / 36
VERTICAL MAGNETIC GRADIENT – RADAR REFLECTIVITY
ABSOLUTE REFLECTIVITY – ZERO MEAN – 0.0-1.0 m

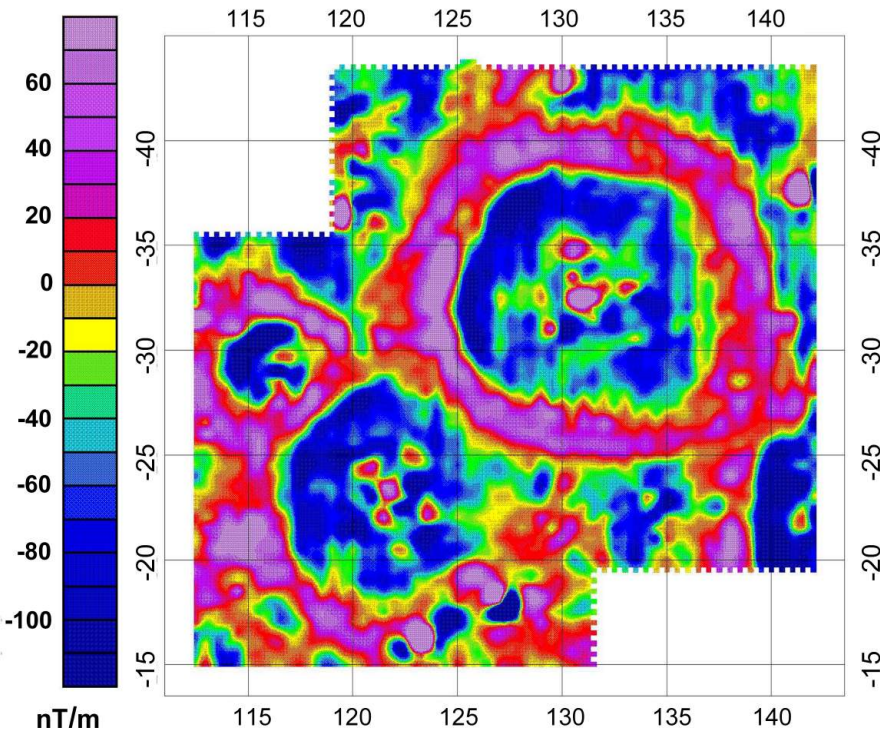
FIGURE:

11

PROJECT: Univ. Montana – Bridge River

DRAWN BY: GMC

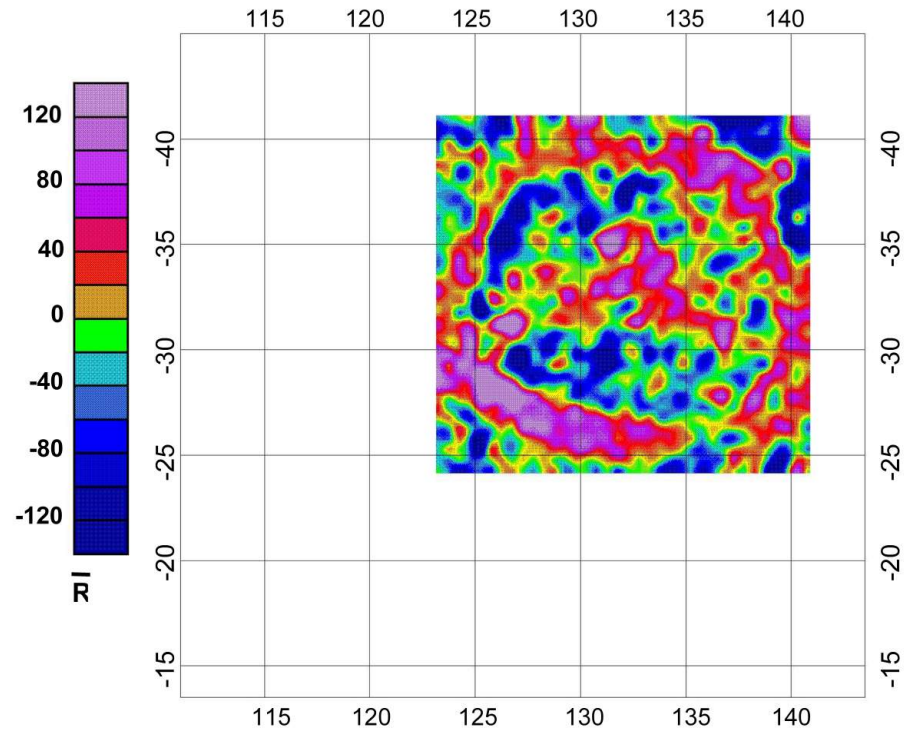
DATE: 27 June, 2005



VERTICAL MAGNETIC GRADIENT

NOTE: Colour scale distributions are approximate and based on interpolation-extrapolation from discrete and time-sampled (GPR) data.

Indicated radar depth levels based on interpreted velocity $v=0.15$ m/ns via diffraction-based velocity estimation.



GROUND RADAR RAW REFLECTIVITY

Raw Reflectivity 13.3 – 26.7 ns (~1.0 – 2.0 m)
 $\Delta x=0.5$ $\Delta y=0.5$
 3x3 Hanning filter (x1)

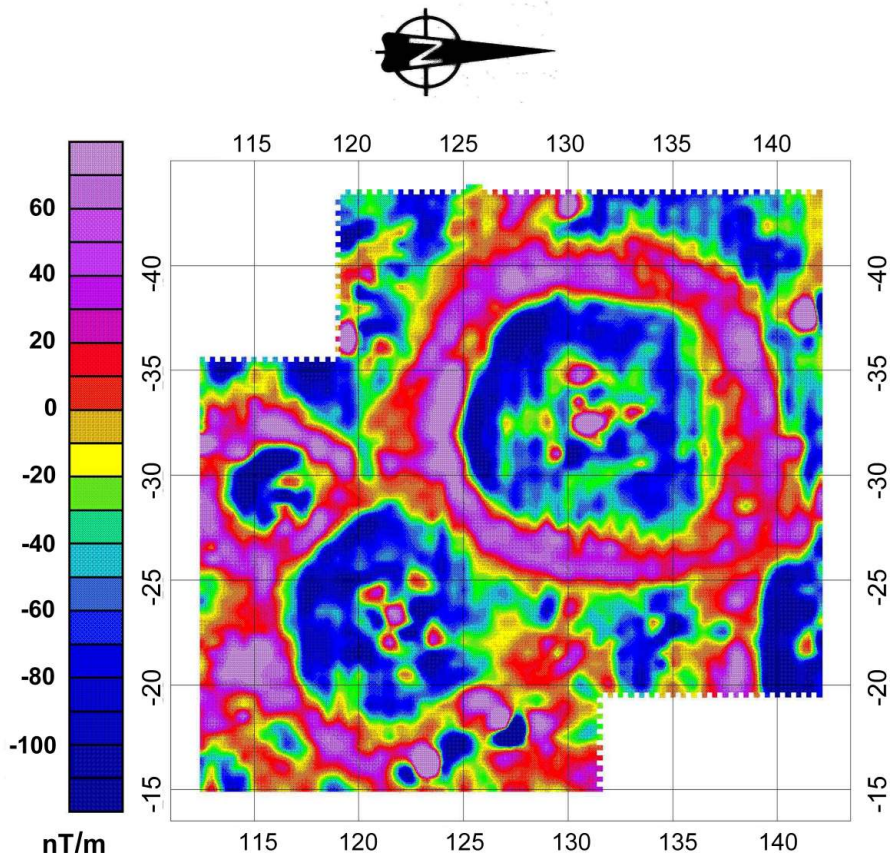


BRIDGE RIVER SITE (EeRI-4) – PIT HOUSES 24 / 36
VERTICAL MAGNETIC GRADIENT – RADAR REFLECTIVITY
RAW REFLECTIVITY – ZERO MEAN – 1.0-2.0 m

PROJECT: Univ. Montana – Bridge River

DRAWN BY: GMC

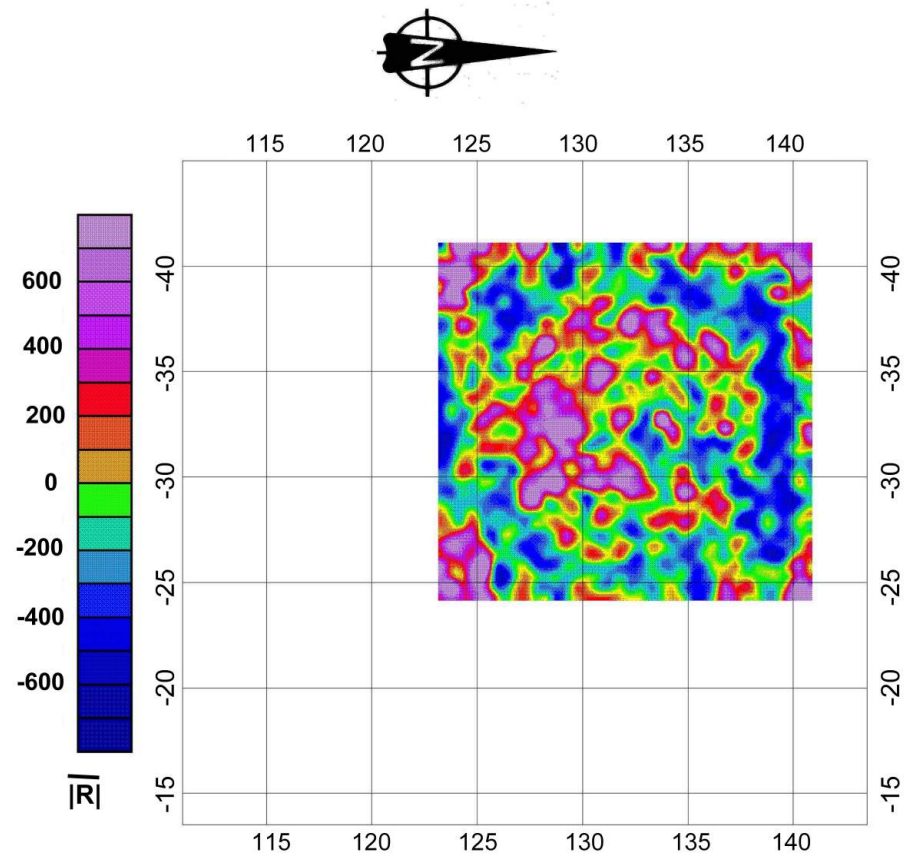
DATE: 27 June, 2005



VERTICAL MAGNETIC GRADIENT

NOTE: Colour scale distributions are approximate and based on interpolation-extrapolation from discrete and time-sampled (GPR) data.

Indicated radar depth levels based on interpreted velocity $v=0.15$ m/ns via diffraction-based velocity estimation.



GROUND RADAR REFLECTIVITY

Absolute Reflectivity 13.3 – 26.7 ns (~1.0 – 2.0 m)
 $\Delta x=0.5$ $\Delta y=0.5$
 3x3 Hanning filter (x1)

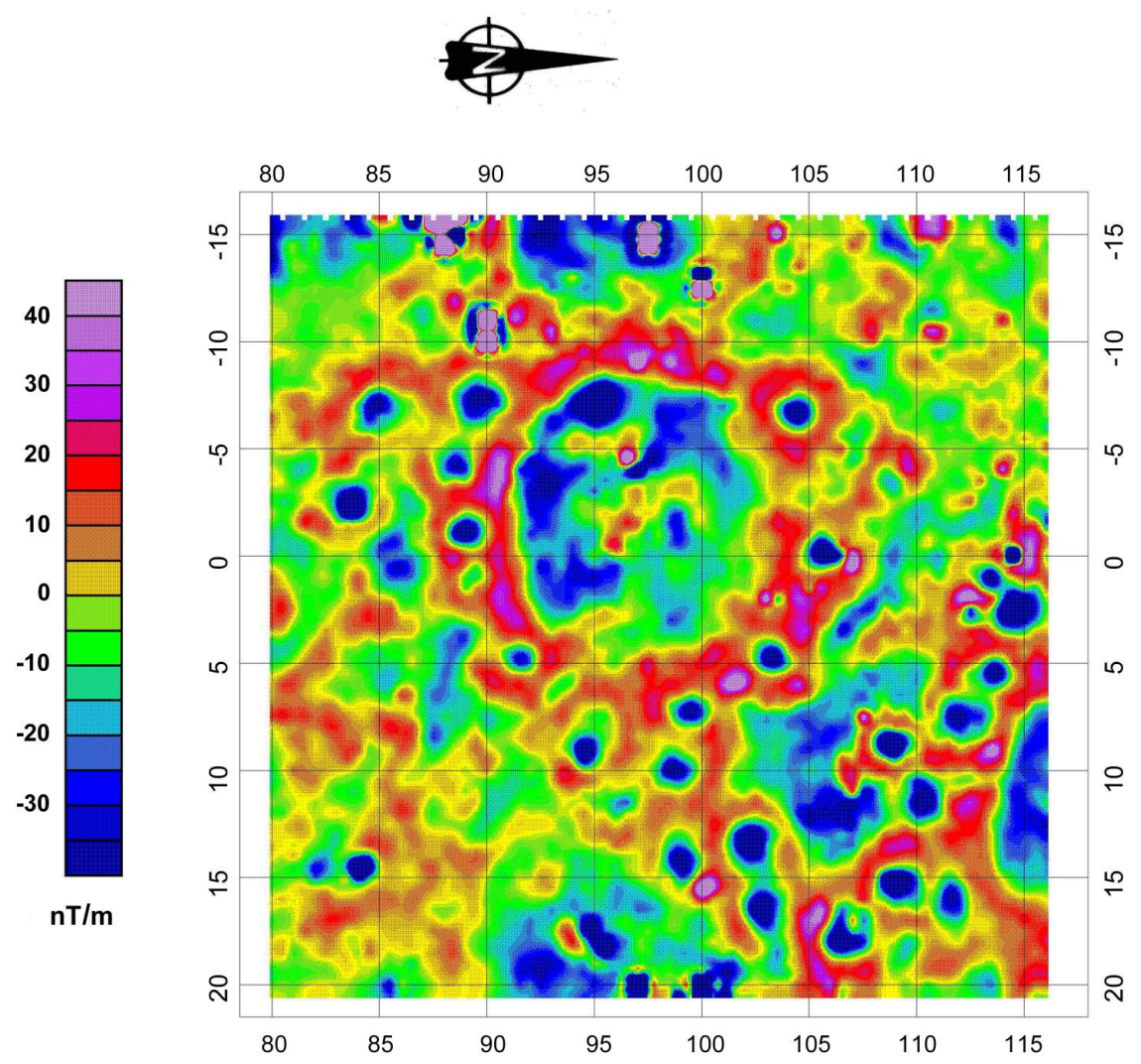


BRIDGE RIVER SITE (EeRI-4) – PIT HOUSES 24 / 36
VERTICAL MAGNETIC GRADIENT – RADAR REFLECTIVITY
ABSOLUTE REFLECTIVITY – ZERO MEAN – 1.0-2.0 m

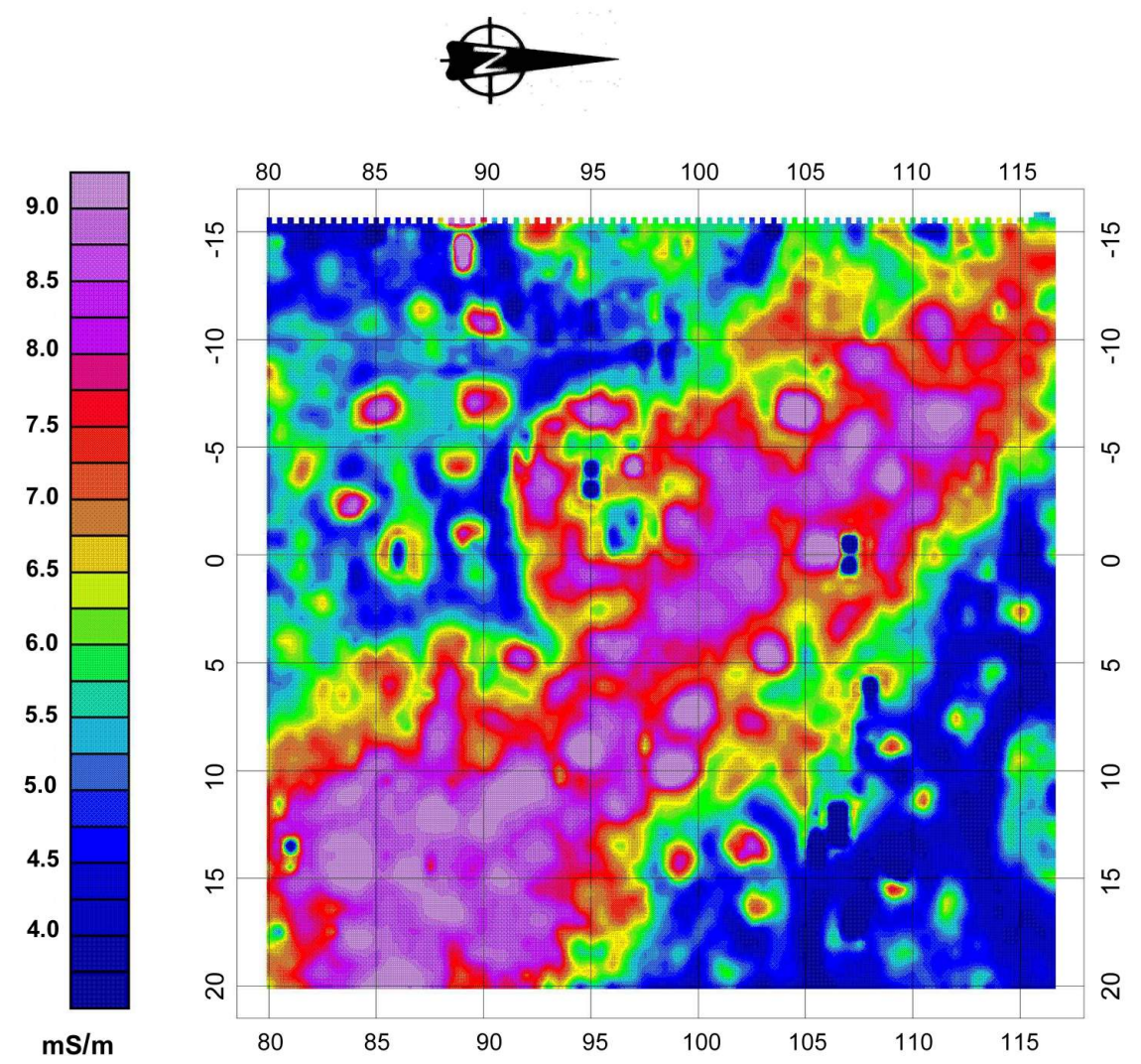
PROJECT: Univ. Montana – Bridge River

DRAWN BY: GMC

DATE: 27 June, 2005



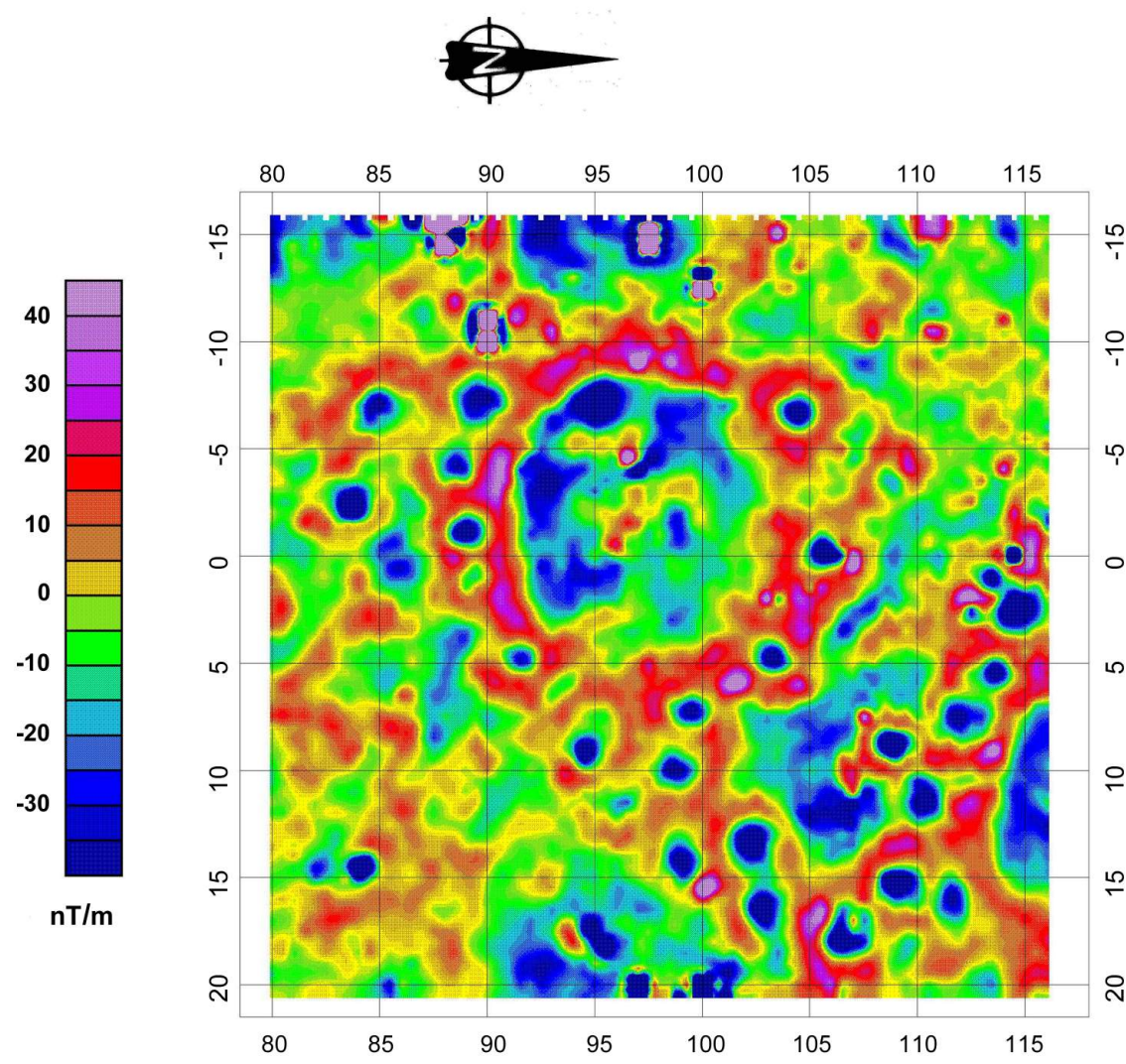
VERTICAL MAGNETIC GRADIENT



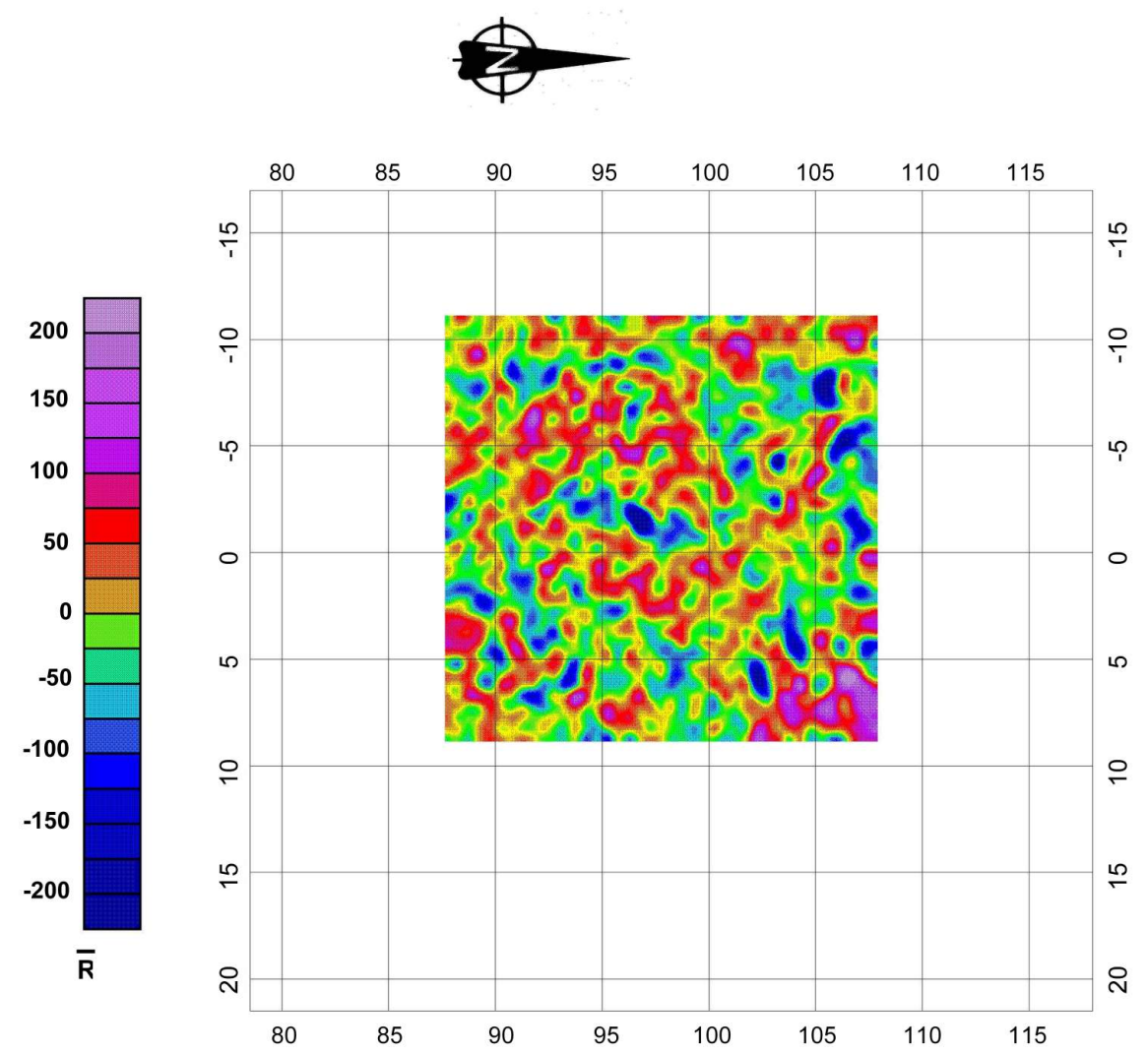
APPARENT ELECTRICAL CONDUCTIVITY

NOTE: Colour scale distributions are approximate and based on interpolation-extrapolation from discrete data.

BRIDGE RIVER SITE (EeRI-4) – PIT HOUSE 20		
VERTICAL MAGNETIC GRADIENT – APPARENT CONDUCTIVITY		
	PROJECT: <i>Univ. Montana – Bridge River</i>	
	DRAWN BY: GMC	FIGURE: 14
	DATE: 26 December, 2004	



VERTICAL MAGNETIC GRADIENT



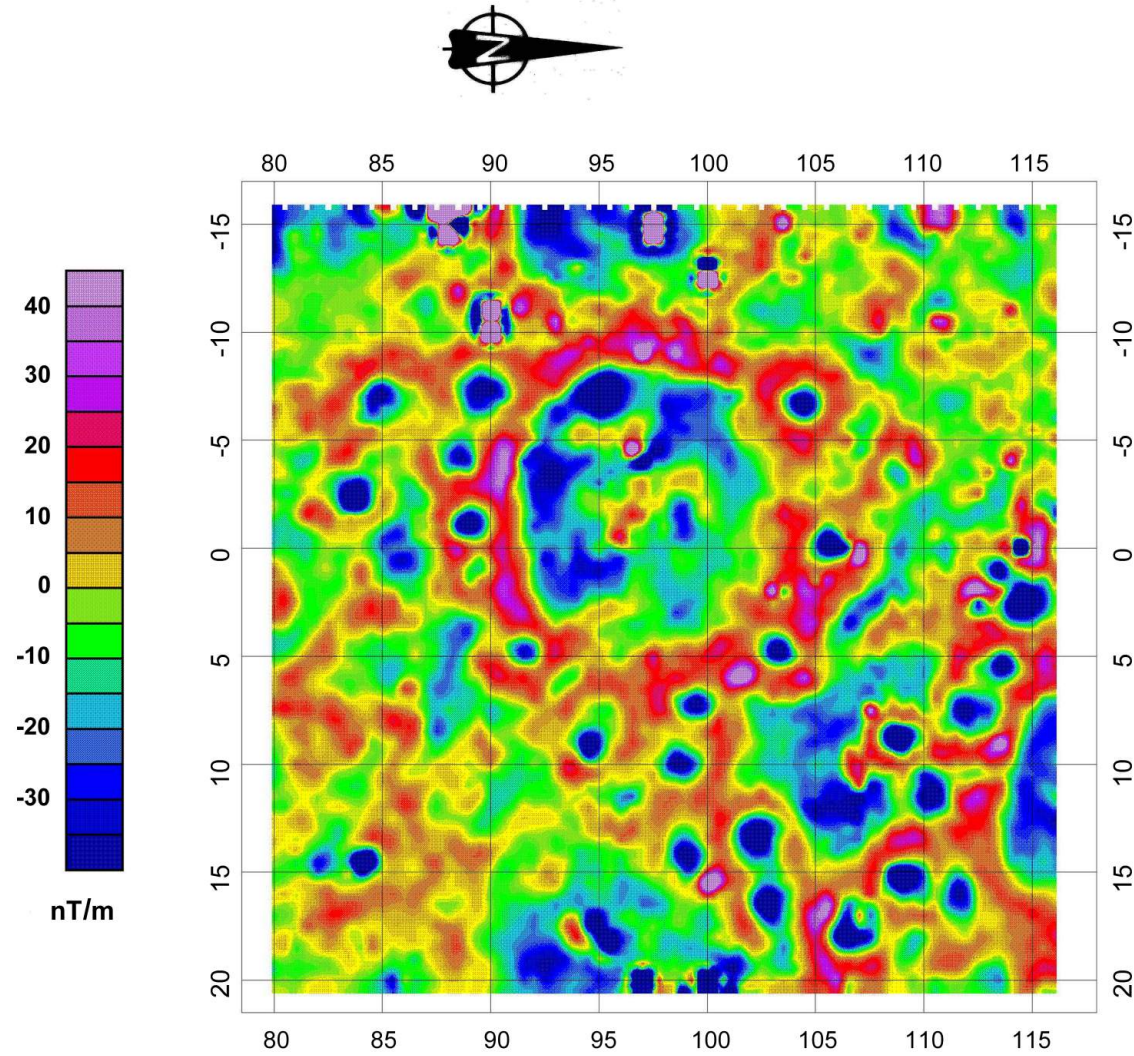
GROUND RADAR RAW REFLECTIVITY

Raw Reflectivity 0.0 – 13.3 ns (~0.0 – 1.0 m)
 $\Delta x=0.5$ $\Delta y=0.5$
 3x3 Hanning filter (x1)

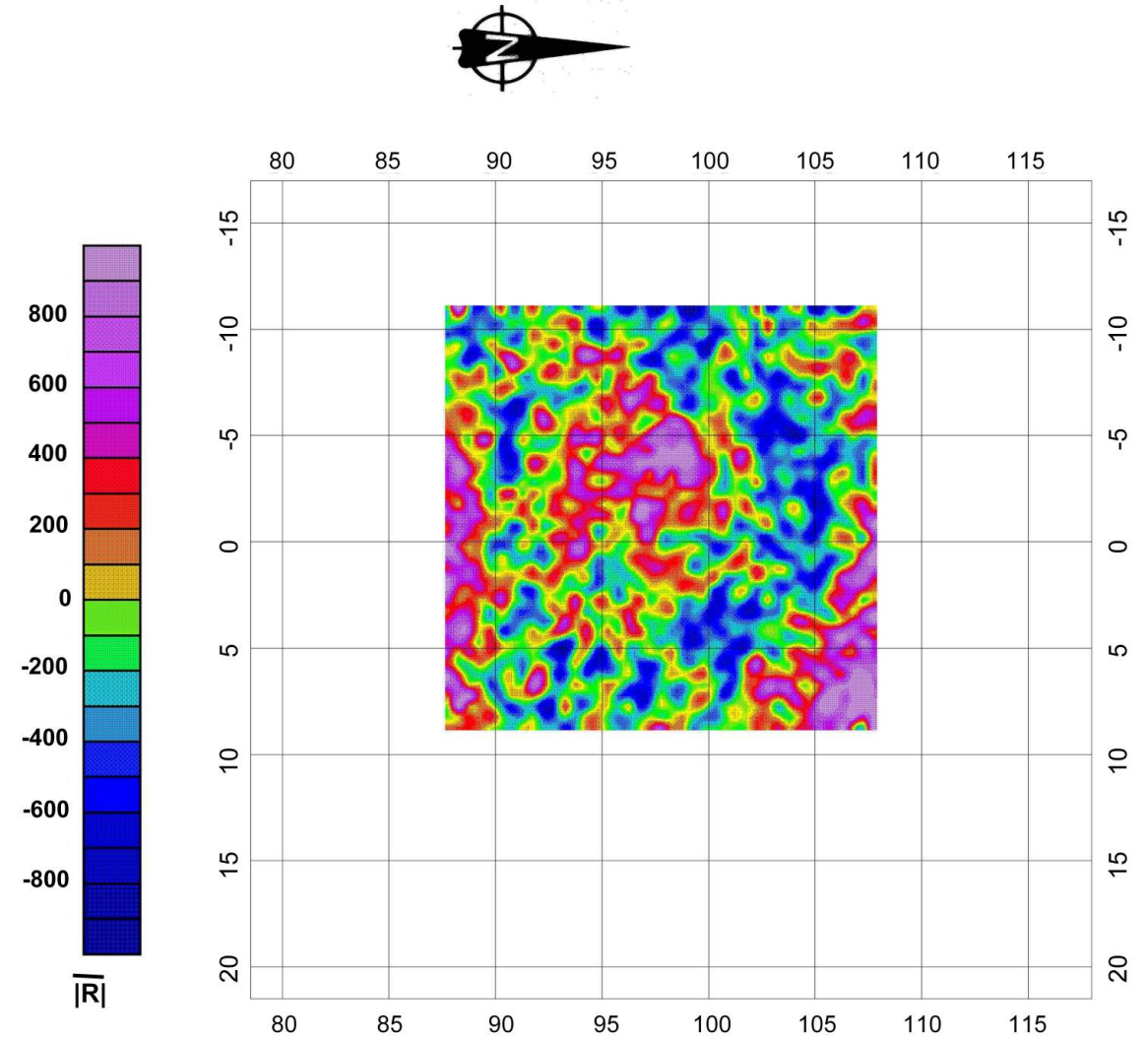
NOTE: Colour scale distributions are approximate and based on interpolation-extrapolation from discrete and time-sampled (GPR) data.

Indicated radar depth levels based on interpreted velocity $v=0.15$ m/ns via diffraction-based velocity estimation.

BRIDGE RIVER SITE (EeRI-4) – PIT HOUSE 20		
VERTICAL MAGNETIC GRADIENT – RADAR REFLECTIVITY		
RAW REFLECTIVITY – ZERO MEAN – 0.0-1.0 m		
	PROJECT: Univ. Montana – Bridge River	
	DRAWN BY: GMC	FIGURE: 15
	DATE: 26 December, 2004	



VERTICAL MAGNETIC GRADIENT



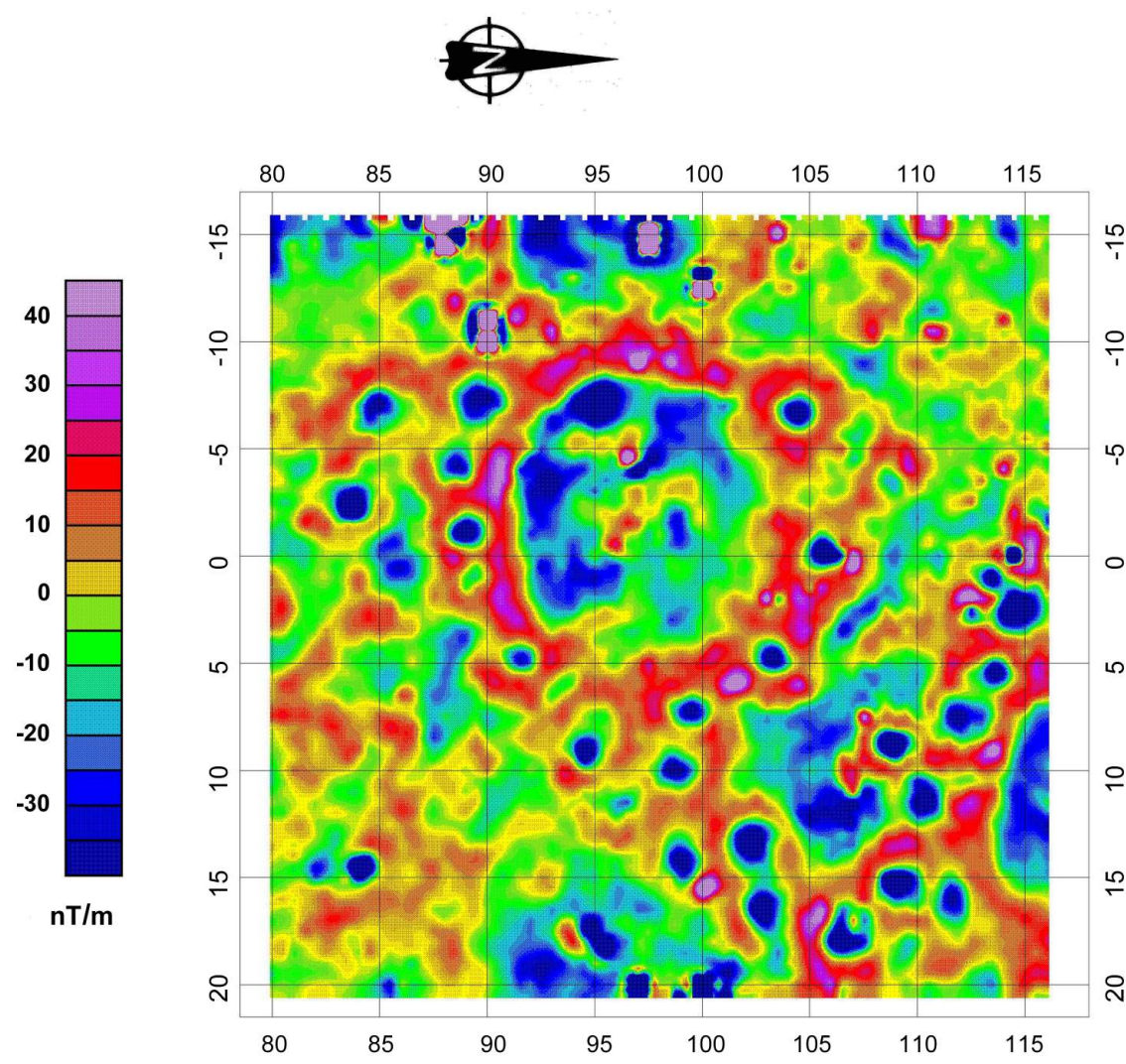
GROUND RADAR ABSOLUTE REFLECTIVITY

Absolute Reflectivity 0.0 – 13.3 ns (~0.0 – 1.0 m)
 $\Delta x=0.5$ $\Delta y=0.5$
 3x3 Hanning filter (x1)

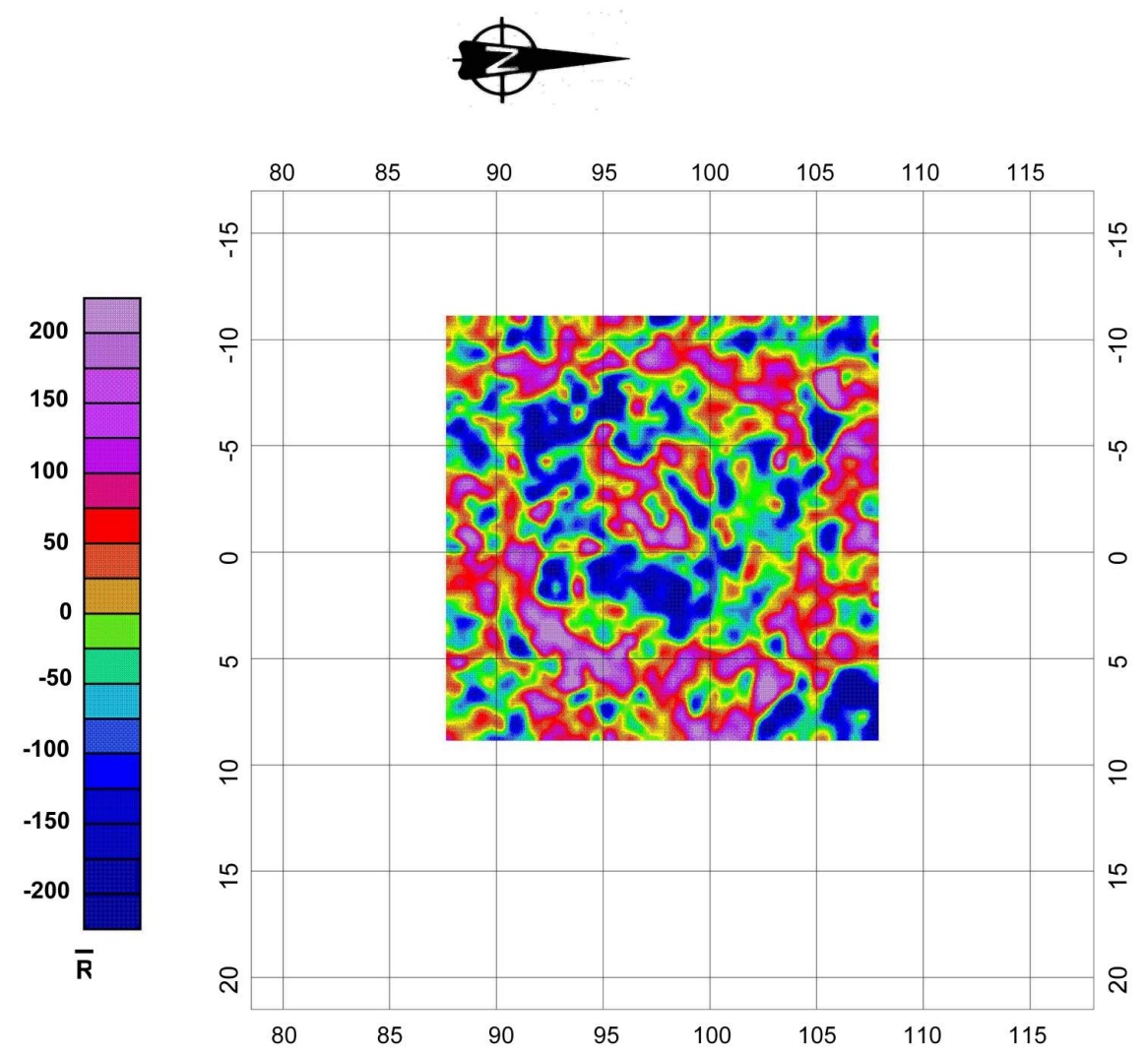
NOTE: Colour scale distributions are approximate and based on interpolation-extrapolation from discrete and time-sampled (GPR) data.

Indicated radar depth levels based on interpreted velocity $v=0.15$ m/ns via diffraction-based velocity estimation.

BRIDGE RIVER SITE (EeRI-4) – PIT HOUSE 20		
VERTICAL MAGNETIC GRADIENT – RADAR REFLECTIVITY		
ABSOLUTE REFLECTIVITY – ZERO MEAN – 0.0-1.0 m		
	PROJECT: <i>Univ. Montana – Bridge River</i>	
	DRAWN BY: GMC	FIGURE: 16
	DATE: 26 December, 2004	



VERTICAL MAGNETIC GRADIENT

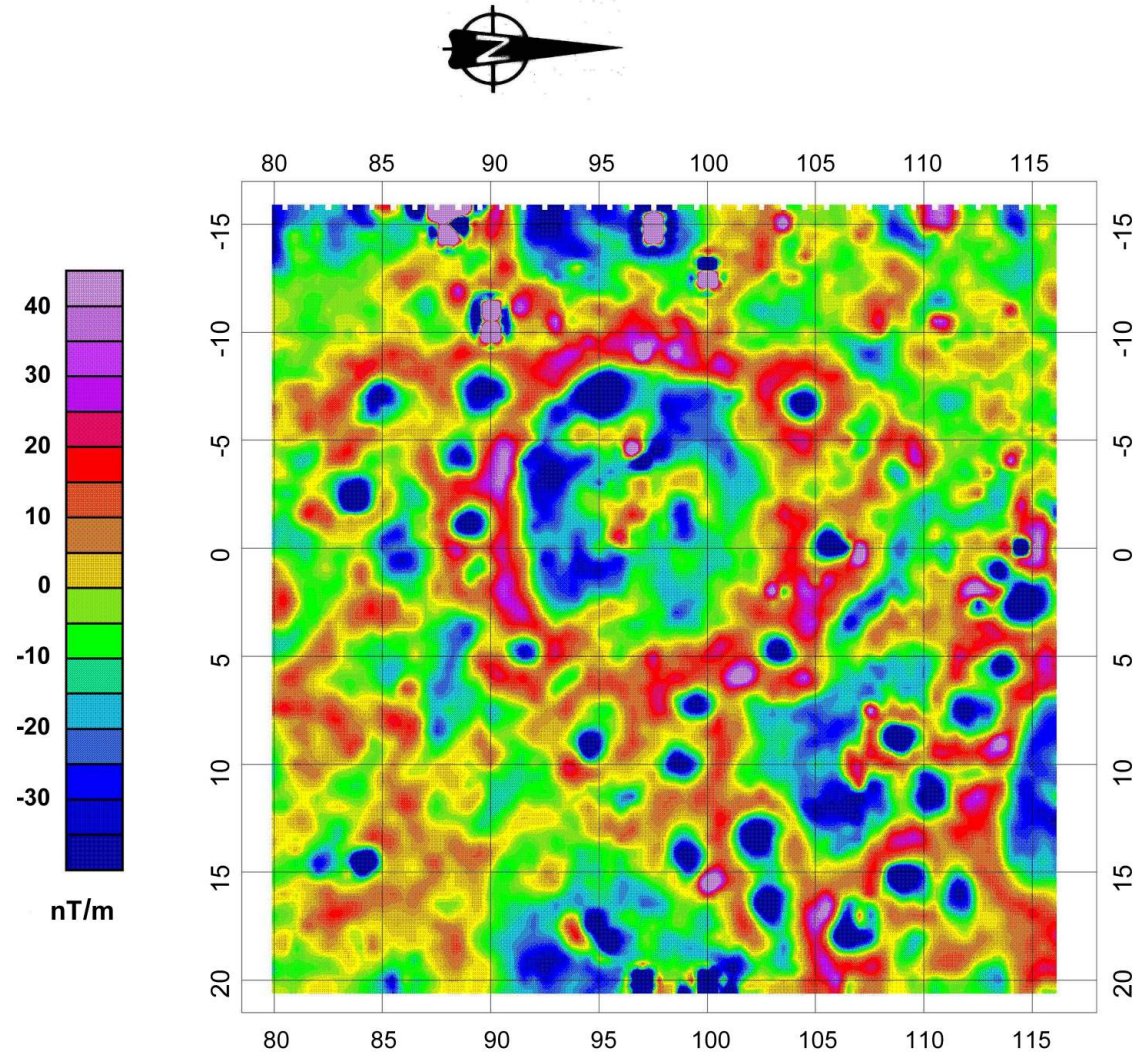


GROUND RADAR RAW REFLECTIVITY
 Raw Reflectivity 13.3 – 26.7 ns (~1.0 – 2.0 m)
 $\Delta x=0.5$ $\Delta y=0.5$
 3x3 Hanning filter (x1)

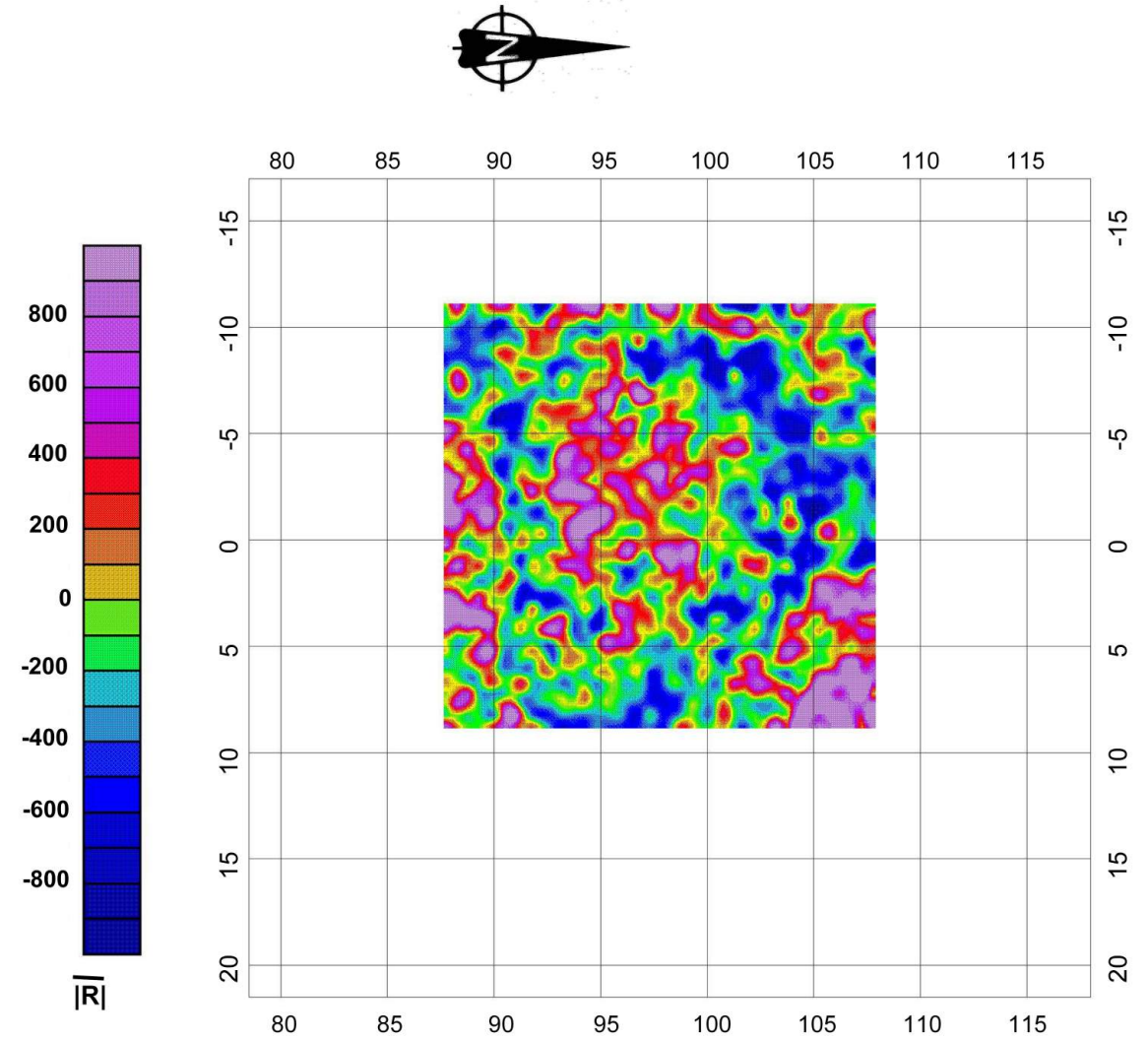
NOTE: Colour scale distributions are approximate and based on interpolation-extrapolation from discrete and time-sampled (GPR) data.

Indicated radar depth levels based on interpreted velocity $v=0.15$ m/ns via diffraction-based velocity estimation.

BRIDGE RIVER SITE (EeRI-4) – PIT HOUSE 20		
VERTICAL MAGNETIC GRADIENT – RADAR REFLECTIVITY		
RAW REFLECTIVITY – ZERO MEAN – 1.0-2.0 m		
	PROJECT: Univ. Montana – Bridge River	
	DRAWN BY: GMC	FIGURE: 17
	DATE: 26 December, 2004	



VERTICAL MAGNETIC GRADIENT



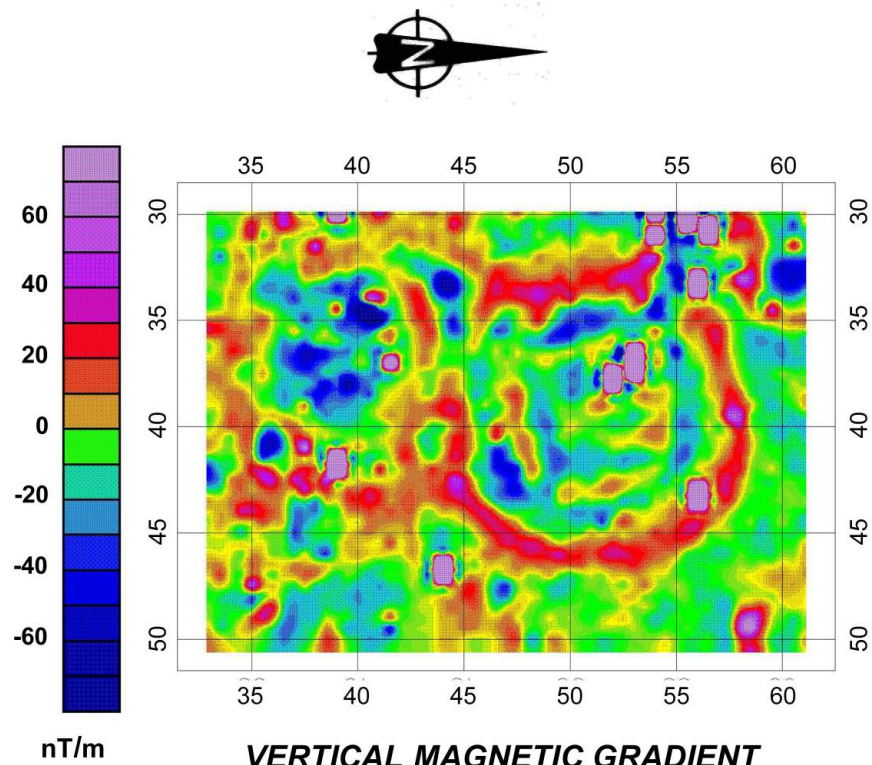
GROUND RADAR ABSOLUTE REFLECTIVITY

Absolute Reflectivity 13.3 – 26.7 ns (~1.0 – 2.0 m)
 $\Delta x=0.5$ $\Delta y=0.5$
 3x3 Hanning filter (x1)

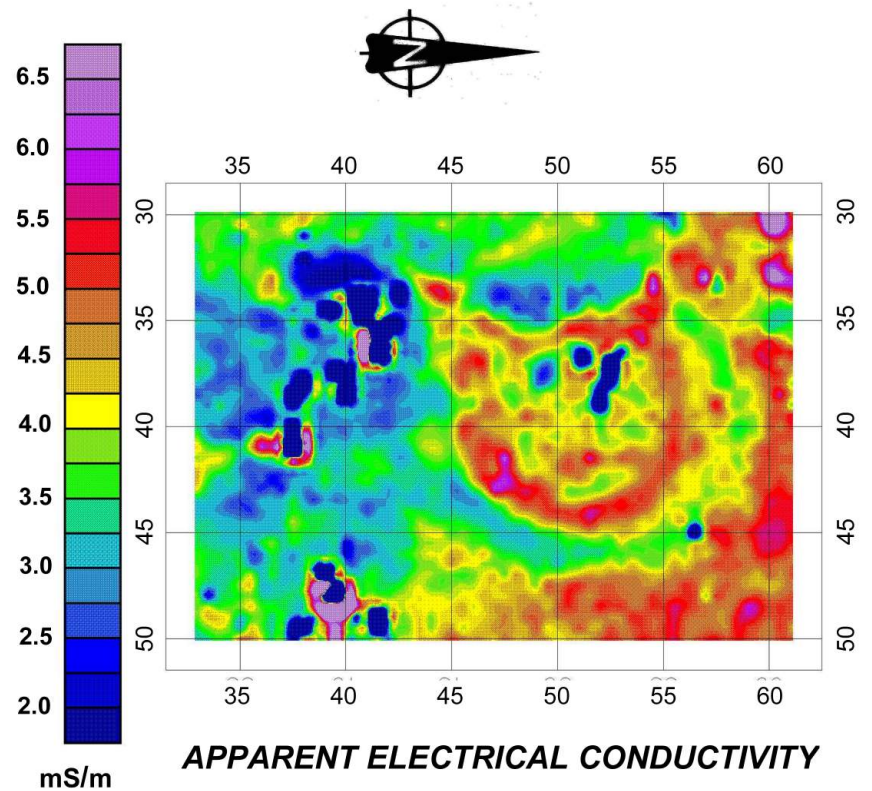
NOTE: Colour scale distributions are approximate and based on interpolation-extrapolation from discrete and time-sampled (GPR) data.

Indicated radar depth levels based on interpreted velocity $v=0.15$ m/ns via diffraction-based velocity estimation.

BRIDGE RIVER SITE (EeRI-4) – PIT HOUSE 20		
VERTICAL MAGNETIC GRADIENT – RADAR REFLECTIVITY		
ABSOLUTE REFLECTIVITY – ZERO MEAN – 1.0-2.0 m		
	PROJECT: <i>Univ. Montana – Bridge River</i>	
	DRAWN BY: GMC	FIGURE: 18
	DATE: 26 December, 2004	



VERTICAL MAGNETIC GRADIENT



APPARENT ELECTRICAL CONDUCTIVITY

NOTE: Colour scale distributions are approximate and based on interpolation-extrapolation from discrete data.



**BRIDGE RIVER SITE (EeRI-4) – PIT HOUSES 10 / 11
VERTICAL MAGNETIC GRADIENT – APPARENT CONDUCTIVITY**

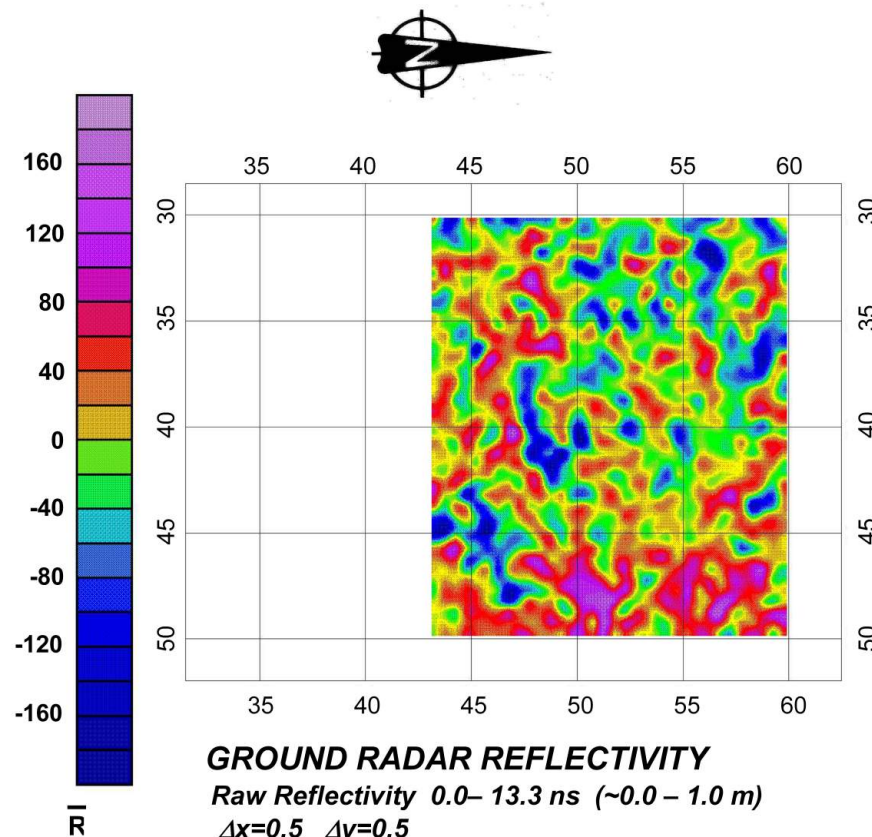
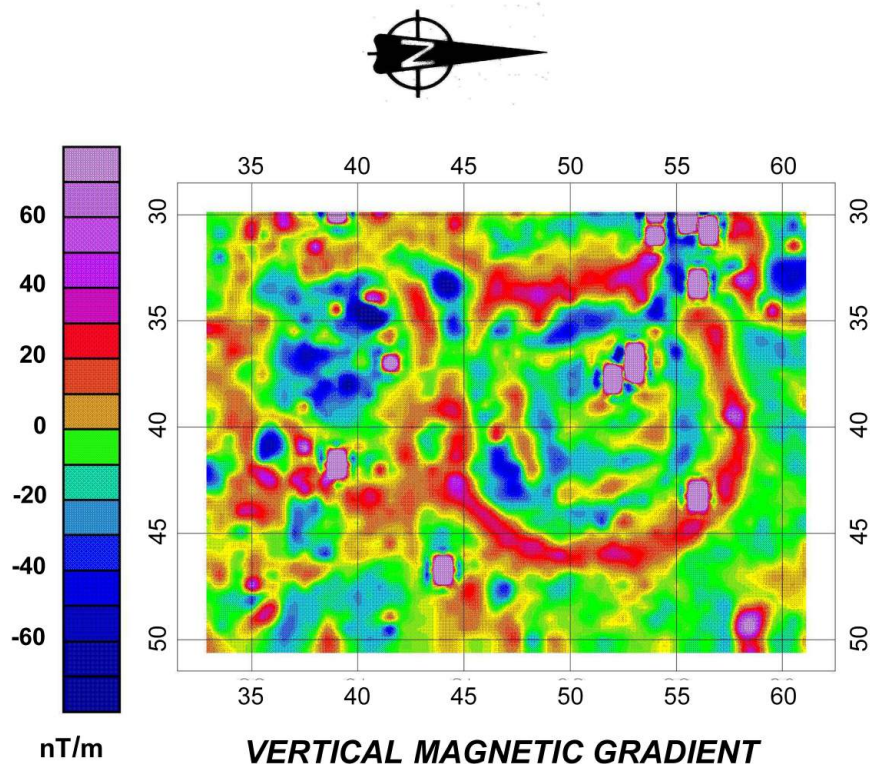
FIGURE:

19

PROJECT: **Univ. Montana – Bridge River**

DRAWN BY: **GMC**

DATE: **5 December, 2004**



NOTE: Colour scale distributions are approximate and based on interpolation-extrapolation from discrete and time-sampled (GPR) data.

Indicated radar depth levels based on interpreted velocity $v=0.15$ m/ns via diffraction-based velocity estimation.

GROUND RADAR REFLECTIVITY

Raw Reflectivity 0.0– 13.3 ns (~0.0 – 1.0 m)

$\Delta x=0.5$ $\Delta y=0.5$

3x3 Hanning filter (x1)



BRIDGE RIVER SITE (EeRI-4) – PIT HOUSES 11
VERTICAL MAGNETIC GRADIENT – RADAR REFLECTIVITY
RAW REFLECTIVITY – ZERO MEAN – 0.0-1.0 m

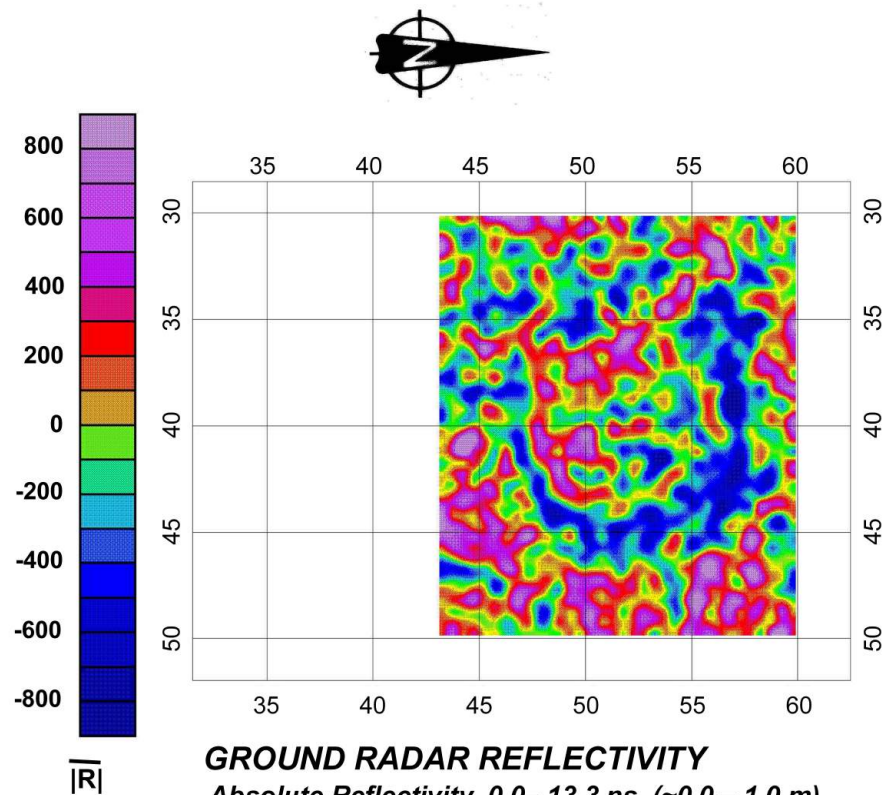
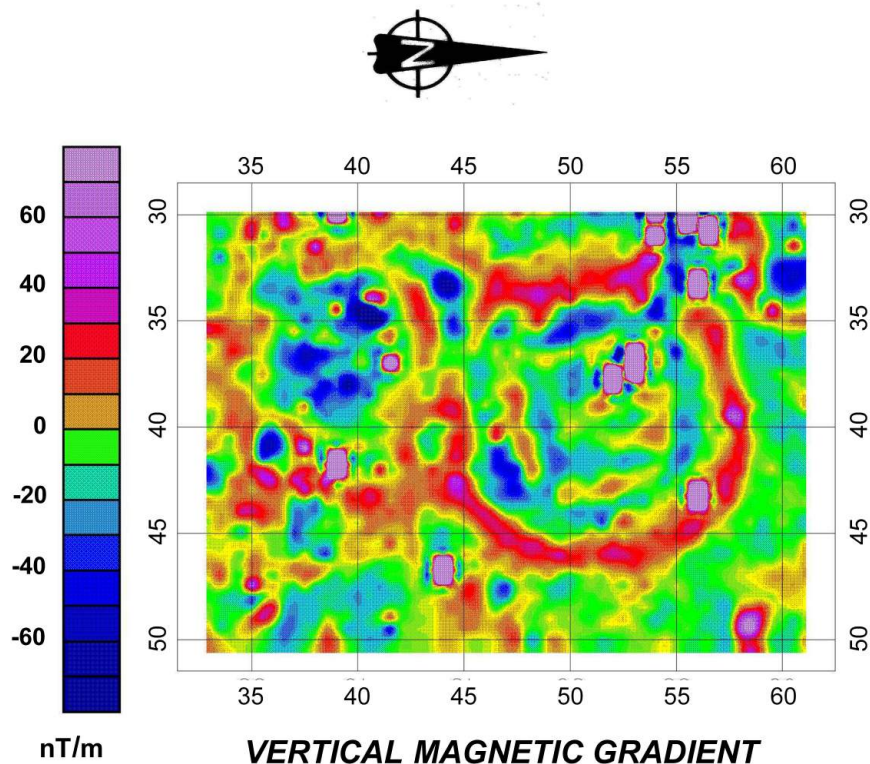
PROJECT: Univ. Montana – Bridge River

DRAWN BY: GMC

DATE: 29 June, 2005

FIGURE:

20



NOTE: Colour scale distributions are approximate and based on interpolation-extrapolation from discrete and time-sampled (GPR) data.

Indicated radar depth levels based on interpreted velocity $v=0.15$ m/ns via diffraction-based velocity estimation.



BRIDGE RIVER SITE (EeRI-4) – PIT HOUSE 11
VERTICAL MAGNETIC GRADIENT – RADAR REFLECTIVITY
ABSOLUTE REFLECTIVITY – ZERO MEAN – 0.0-1.0 m

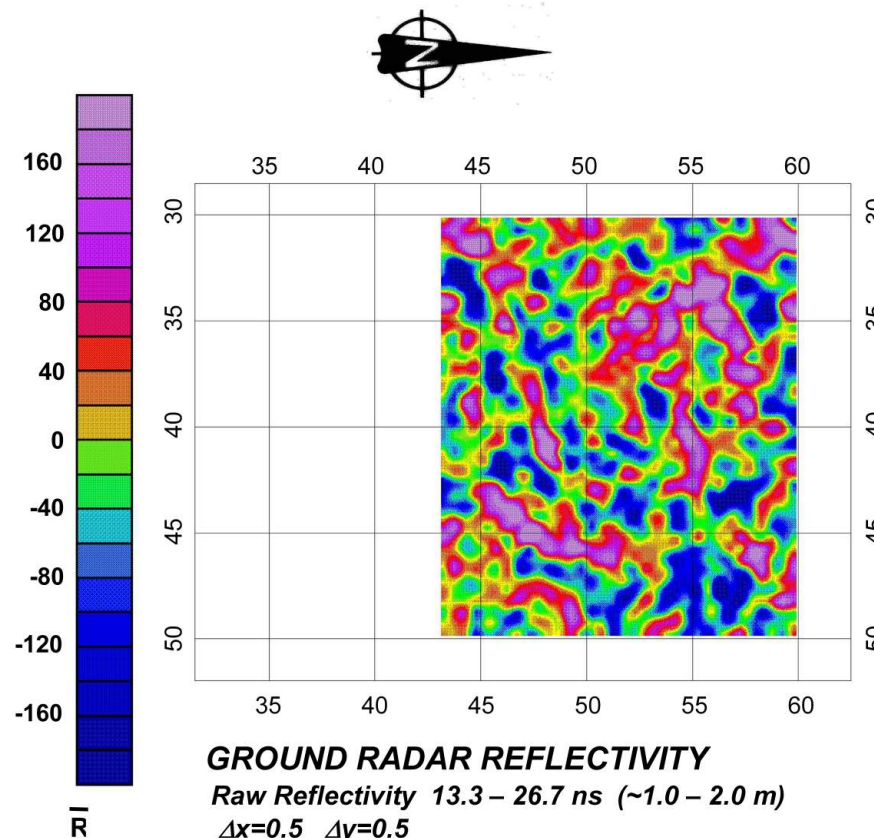
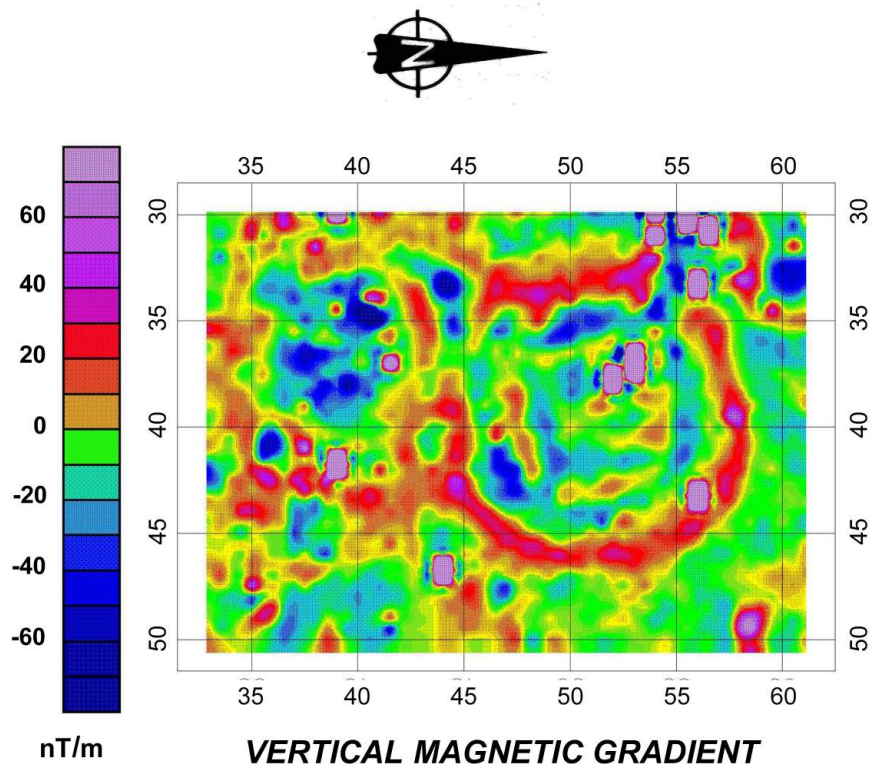
FIGURE:

21

PROJECT: Univ. Montana – Bridge River

DRAWN BY: GMC

DATE: 29 June, 2005



NOTE: Colour scale distributions are approximate and based on interpolation-extrapolation from discrete and time-sampled (GPR) data.

Indicated radar depth levels based on interpreted velocity $v=0.15$ m/ns via diffraction-based velocity estimation.

GROUND RADAR REFLECTIVITY

Raw Reflectivity 13.3 – 26.7 ns (~1.0 – 2.0 m)

$\Delta x=0.5$ $\Delta y=0.5$

3x3 Hanning filter (x1)



BRIDGE RIVER SITE (EeRI-4) – PIT HOUSES 11
VERTICAL MAGNETIC GRADIENT – RADAR REFLECTIVITY
RAW REFLECTIVITY – ZERO MEAN – 1.0-2.0 m

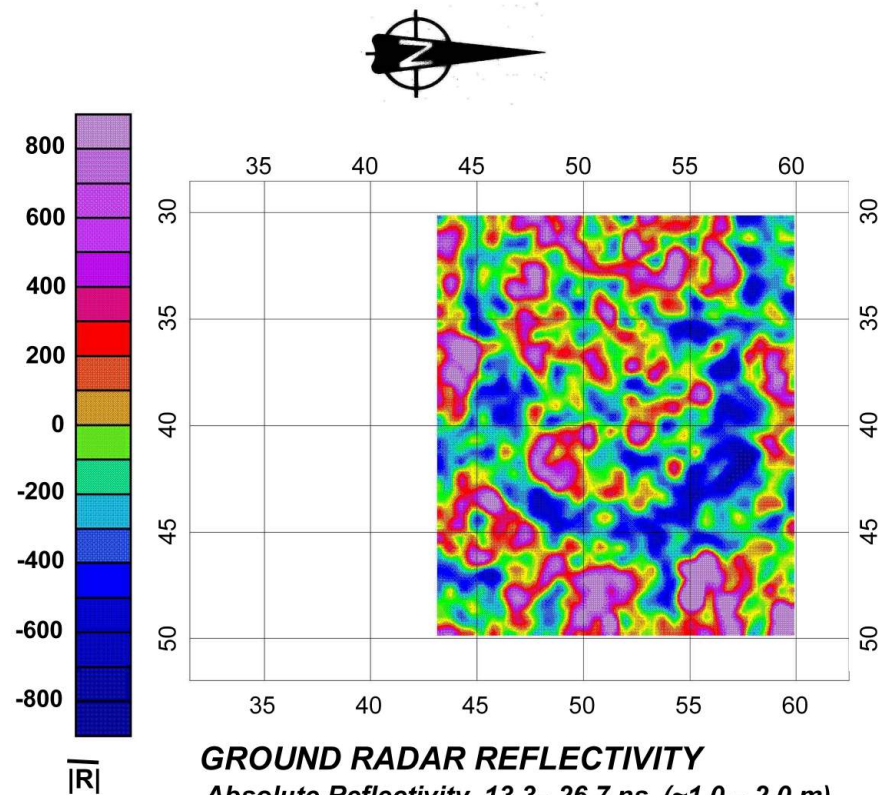
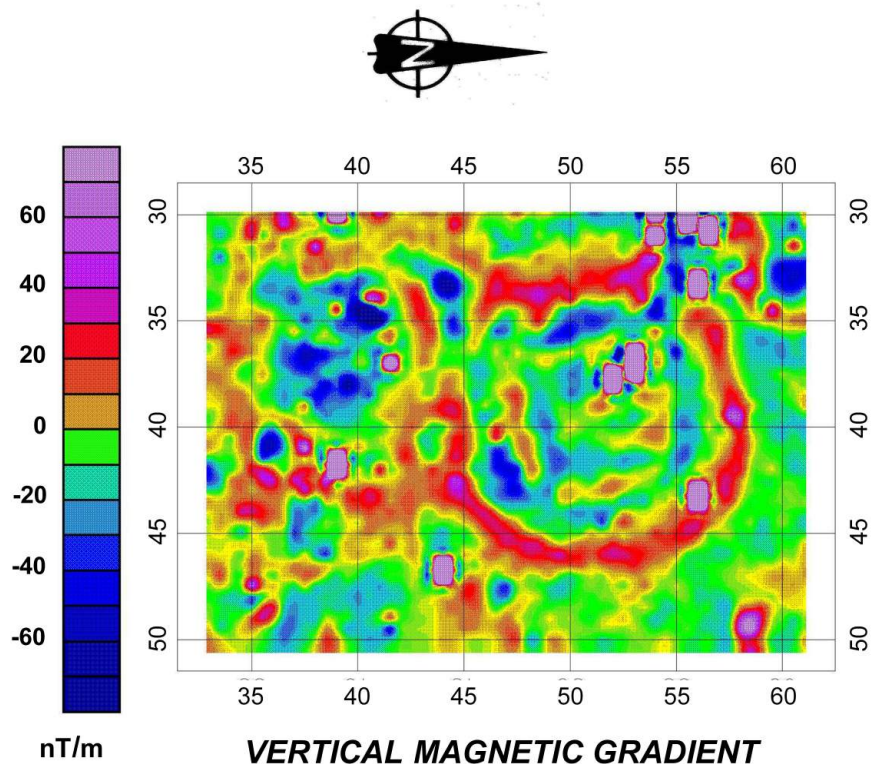
FIGURE:

22

PROJECT: Univ. Montana – Bridge River

DRAWN BY: GMC

DATE: 29 June, 2005



NOTE: Colour scale distributions are approximate and based on interpolation-extrapolation from discrete and time-sampled (GPR) data.

Indicated radar depth levels based on interpreted velocity $v=0.15$ m/ns via diffraction-based velocity estimation.

GROUND RADAR REFLECTIVITY
 Absolute Reflectivity 13.3– 26.7 ns (~1.0 – 2.0 m)
 $\Delta x=0.5$ $\Delta y=0.5$
 3x3 Hanning filter (x1)



BRIDGE RIVER SITE (EeRI-4) – PIT HOUSES 11
VERTICAL MAGNETIC GRADIENT – RADAR REFLECTIVITY
ABSOLUTE REFLECTIVITY – ZERO MEAN – 1.0-2.0 m

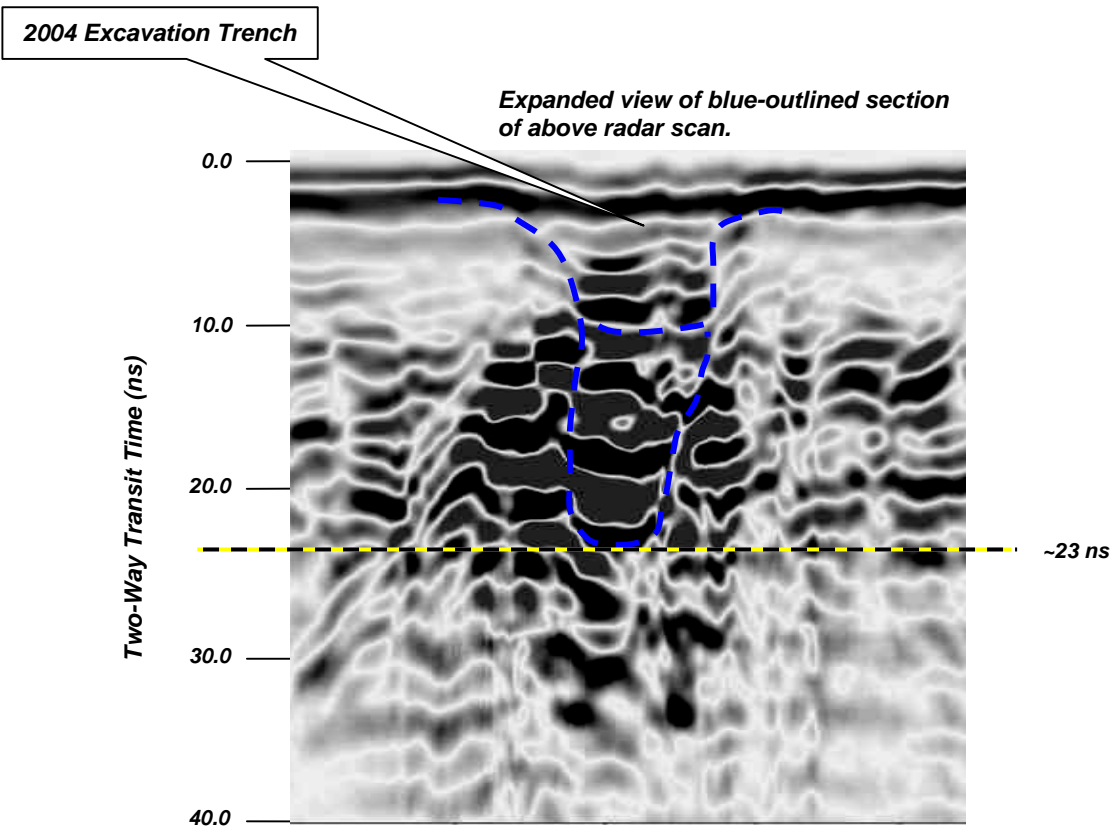
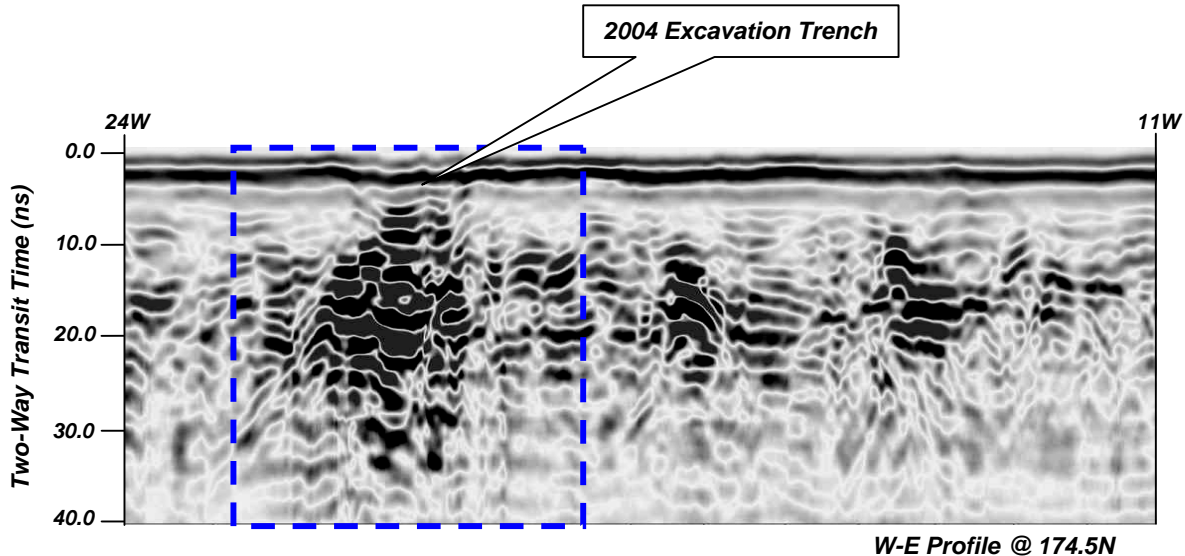
FIGURE:

23

PROJECT: Univ. Montana – Bridge River

DRAWN BY: GMC

DATE: 29 June, 2005



NOTE: Assumed total depth of excavations at 1.8 m implies an approximate radar velocity $v=0.15$ m/ns. This value is consistent with data-based velocity estimates.

**BRIDGE RIVER SITE (EeRI-4)
GROUND RADAR – HP54 – 2004 EXCAVATION TRENCH**



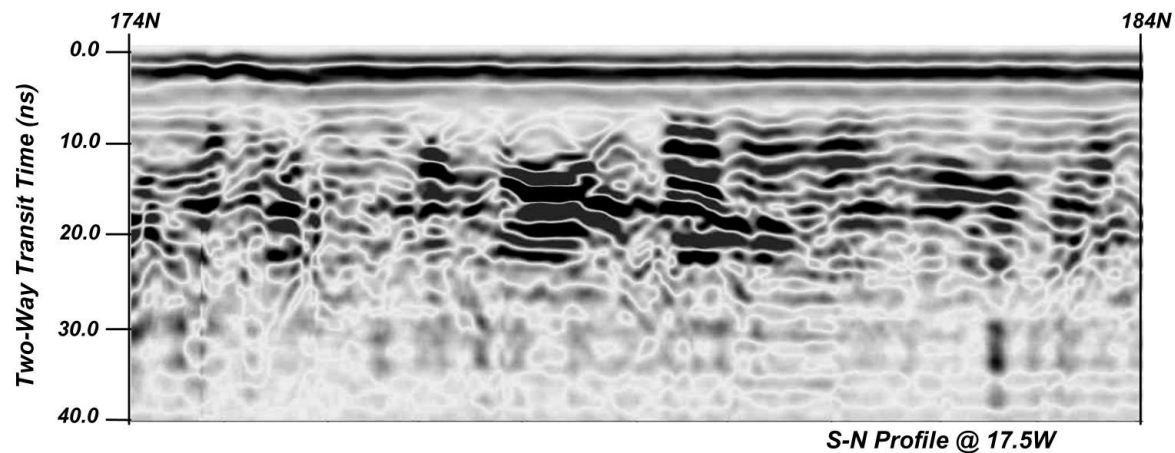
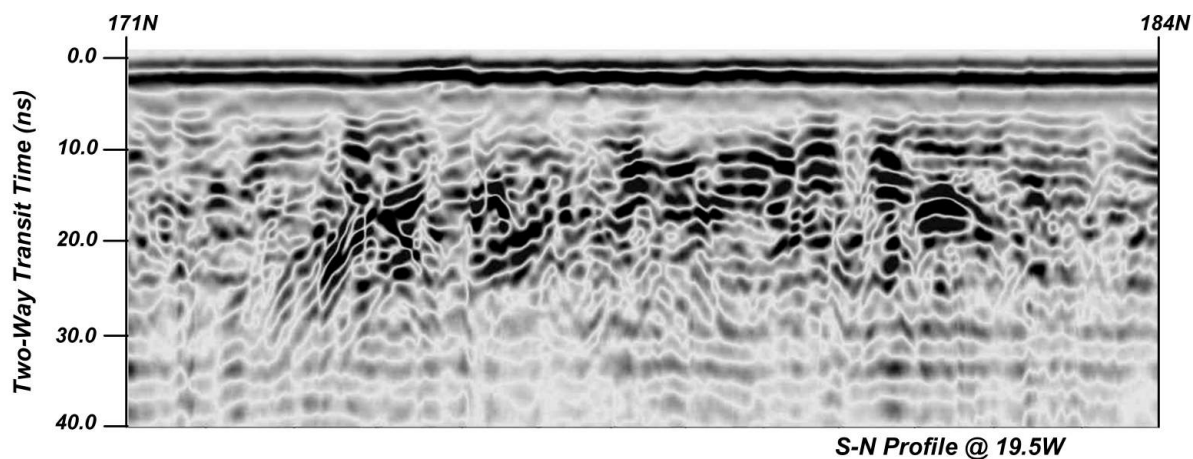
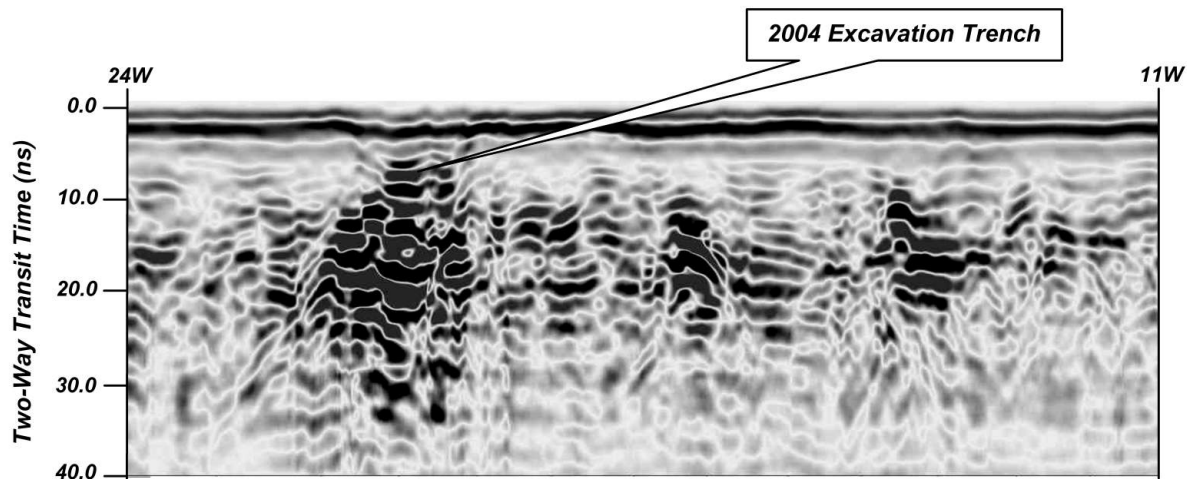
PROJECT: Univ. Montana – Bridge River

FIGURE:

DRAWN BY: GMC

DATE: 12 October, 2004

24



**BRIDGE RIVER SITE (EeRI-4)
GROUND RADAR SCANS – HP54**



PROJECT: Univ. Montana – Bridge River

FIGURE:

DRAWN BY: GMC

DATE: 12 October, 2004

25